

On Outage-based Beamforming Design for Dual-Functional Radar-Communication 6G Systems

Ahmad Bazzi and Marwa Chafii

Abstract—This article studies and derives beamforming waveform designs in a dual-functional radar-communication (DFRC) multiple-input-multiple-output system. We focus on a scenario, where the DFRC base station communicates with downlink communication users, with imperfect channel state information knowledge, and performs target detection, all via the same transmit waveform. Through careful relaxation procedures, we arrive at a suitable and novel optimization problem, which maximizes the radar output power in the Bartlett sense, under probabilistic outage signal-to-interference-and-noise ratio constraints. Theoretical analysis proves optimality of the solution given by the relaxed version of the problem, as well as closed-form solutions in certain scenarios. Finally, the achieved performances and trade-offs of the proposed beamforming design are demonstrated through numerical simulations.

Index Terms—joint sensing and communications, integrated sensing and communications, beamforming, waveform design, 6G

I. INTRODUCTION

6G is expected to nurture a wide scope of services, spanning haptic telemedicine to VR/AR remote services and holographic teleportation with massive eXtended reality (XR) capabilities, as well as Blockchain [1], just to name a few. The benefits of 6G go beyond communication. It will incorporate new capabilities like sensing and computing, allowing new services and utilizing improved environmental information for machine learning and artificial intelligence. On the other hand, such bandwidth-hungry applications require a $10^3 \times$ capacity increase, as highlighted by [2]. Even more, the monthly mobile data per mobile broadband subscriber is expected to grow from 5.3 GB, by 2020, to 257 GB by 2030, which is a $50 \times$ increase within a decade [3].

Indeed, integrated sensing and communications cooperation [5] and convergence [6] is an utmost topic that will serve as a door-opener for innovative applications like never seen before, such as autonomous driving [4], robotics and UAV sector. Consequently, coexistence between radar and communication systems [7] has been a primary field of investigation¹. Joint sensing and communication comes with a number of practical advantages, an obvious one being spectrum efficiency, due to the interoperability between the radar and communication counterparts. Another advantage on the table is hardware

Ahmad Bazzi is with the Engineering Division, New York University (NYU) Abu Dhabi, 129188, UAE (email: ahmad.bazzi@nyu.edu).

Marwa Chafii is with Engineering Division, New York University (NYU) Abu Dhabi, 129188, UAE and NYU WIRELESS, NYU Tandon School of Engineering, Brooklyn, 11201, NY, USA (email: marwa.chafii@nyu.edu).

¹Not to be mistaken with radar-communication coexistence, which is distinct from integrated sensing and communication. See [8] for more details.

resource sharing between radar and communication tasks, thus having both on a single platform will lead to reduced PHY-layer modem size and cost. With these merits come a serious number of challenges and research questions that need to be addressed, such as efficient resource reuse and spectrum sharing [9], [10], trade-offs between high communication rates and high-resolution sensing performances [11]–[13], privacy and security [16], shared waveform design [14], [15], [24]. In this article, we focus on waveform beamforming design, so as to achieve a single waveform for both communication and sensing tasks.

Heretofore, previous beamforming design for joint radar and communications have been conducted under perfect channel state information (CSI). Even though CSI may be estimated between the dual-functional radar-communication (DFRC) base station and the communication users², the CSI cannot be perfect. A main driver of this inaccurate knowledge comes from hardware imperfections [21]. For instance, quantization errors which is caused by analog-to-digital converters (ADCs) within the RF-Frontend of the PHY modem, will further lead to estimation errors, which in turn leads to fixed-point error propagation. From a hardware perspective, it is highly desired to economize the total bit width of the baseband design. This need serves as key motivation behind sophisticated baseband modems, that are aware of imperfect CSI. Joint communication and sensing DFRC modems will not be an exception.

On the other hand, beamforming with imperfect CSI knowledge has been considered in different scenarios. For example, one of three use cases in [16] assumes imperfect CSI and directional information; however, the problem is to minimize the signal-to-noise ratio (SNR) towards an eavesdropper with some information about its position, while guaranteeing a given SINR towards legitimate users. This is achieved via artificial noise statistics. Another robust approach with imperfect CSI was addressed in [17] where the probability of radar detection, under a radar-communication interference channel, is the central cost to be maximized, subject to acceptable SINR constraints for different communication users. Furthermore, the problems in [16], [17] have adopted the so-called \mathcal{S} -procedure, which leads to a tractable convex optimization problem. Moreover, [18] considers an imperfect CSI coming from inaccurate knowledge of transmit powers; hence, a mismatch in the computation of the LMMSE receiver. Robust beamforming has also been employed in other contexts, such

²CSI acquisition may be done via one-way where users send a training sequence assuming channel reciprocity, or two-way where DFRC base station sends a sequence, then channel estimation is done per user and fed back to the base station

as high-mobility downlink scenarios [19] and worst-case analysis for conservative-type robust beamforming [20].

Unlike previous works on joint communications and sensing that consider perfect CSI with deterministic SINR, we propose in this paper a new optimization framework for DFRC taking into account outage SINR probability. To the best of our knowledge, outage SINR probability considerations, and therefore the achievable trade-offs, in the context of joint sensing and communications have not been addressed, yet. In the following two subsections, we highlight novel contributions and shed light on some important insights appearing in this manuscript.

A. Contributions and Insights

The paper considers dual-function radar communication beamforming towards communication users, while scanning targets in specific directions. Due to the imperfect CSI case, our precoding scheme aims at optimizing weight vectors to guarantee a maximal outage SINR level, while maximizing the power of the radar beamformer in the desired look-direction, through the Bartlett criterion. The initial problem involves stochastic constraints, which are then transformed to deterministic forms through a series of carefully chosen relaxations. To this end, we summarize our contributions as follows

- **DFRC beamforming design with imperfect CSI.** We propose a dual-functional radar-communication beamforming design at the base station in the downlink, in the case of imperfect channel state information.
- **Constraint relaxations towards a convex DFRC beamforming design.** We formulate a novel convex optimization problem, thanks to a series of careful relaxations, for designing dual-functional beamformed waveforms that offer enormous tradeoff advantages between communication achievable rates and different radar metrics, such as the probability of detection and integrated-sidelobe-to-mainlobe-ratio (ISMR).
- **Proof of rank-one beamforming solutions.** We prove rank-one optimality of the final relaxed version of the beamforming optimization problem, a property that is highly desired when a rank relaxation has been imposed at some point of an optimization problem. Indeed, this property has the advantage of guaranteeing exact beamforming vectors, rather than just mere approximations used to generate an approximate rank-one solution, thus ruling-out the need of a postprocessing method to generate such weight vectors.
- **Closed-form solutions of DFRC beamforming design.** We derive closed-form solutions of the dual-functional beamforming design problem in the single-user (SU) case. Thanks to the derived expressions, we bring novel insights into the achievable radar-communication trade-offs via the involved hyperparameters of the optimization problem in hand.
- **Radar-Communication trade-offs.** Simulation results show that radar-communication trade-offs not only exist for several key metrics, but also offer better achievable

joint radar-communication performances, as compared to existing waveform designs.

Furthermore, we reveal some important insights, i.e.

- Closed-form solutions reveal the explicit dependencies of outage parameters on the radar-communications trade-off. The level of correlation between the steering vector towards the target and the channel between the DFRC base station and the communication user also has a direct impact on this trade-off. Graphical interpretations are also given to illustrate this point.
- The accuracy of the resulting radar's beam pattern in the desired look-direction depends on the SINR outage threshold, in the presence of imperfect CSI. In other words, the higher the SINR we target, the less capable the radar is in looking at certain directions. Likewise, the radar's sidelobe rejection also depends on the target SINR.
- Under a unit transmit power constraint, the proposed design could achieve an average sum-rate of 4.78 bits/sec/Hz/user with a probability of detection of ~ 0.99 , as compared to ~ 0.65 when state-of-the-art methods are adopted [24]. Interpretation on such radar gains are given in the simulations section.
- For a fixed ISMR level, the average achievable rate increases with a decrease in number of communication users or an increase in the desired SINR outage threshold.

B. Organization and Notations

The rest of this paper is organized as follows. We introduce the system model for radar and communications, as well as some KPIs, in Section II. The proposed DFRC beamforming design with imperfect CSI is derived in Section III. Section IV presents extensive simulation results, and Section V concludes the paper.

Notation: Upper-case and lower-case boldface letters denote matrices and vectors, respectively. $(\cdot)^T$, $(\cdot)^*$ and $(\cdot)^H$ represent the transpose, the conjugate and the transpose-conjugate operators. The statistical expectation is denoted as $\mathbb{E}\{\cdot\}$. The vectorization and unvectorization operators are denoted as vec and vec^{-1} , respectively. In particular, vec takes an $N \times M$ matrix \mathbf{X} as input and returns an $NM \times 1$ vector, by stacking the columns of \mathbf{X} one on top of the other. For any complex number $z \in \mathbb{C}$, the magnitude is denoted as $|z|$, its angle is $\angle z$, and its real part is $\text{Re}(z)$. The Frobenius norm of matrix \mathbf{X} is denoted as $\|\mathbf{X}\|$. We denote a positive semi definite matrix as $\mathbf{X} \succeq \mathbf{0}$ and $\lambda_{\max}(\mathbf{X})$ is the maximum eigenvalue of matrix \mathbf{X} . The matrix \mathbf{I}_N is the identity matrix of size $N \times N$. The zero-vector is $\mathbf{0}$. The rank returns the rank of a matrix and Tr returns the trace of a matrix. The inverse of a square matrix is \mathbf{X}^{-1} . The probability of an event \mathcal{A} is $\text{Pr}(\mathcal{A})$. The span of vectors $\mathbf{x}_1 \dots \mathbf{x}_N$ is $\text{span}\{\mathbf{x}_1 \dots \mathbf{x}_N\}$. The noncentral chi-squared distribution function with n degrees of freedom and parameter ρ is denoted as $\mathcal{F}_{\chi_n^2(\rho)}$ and the central chi-squared distribution with n degrees of freedom is denoted as $\mathcal{F}_{\chi_n^2}$.

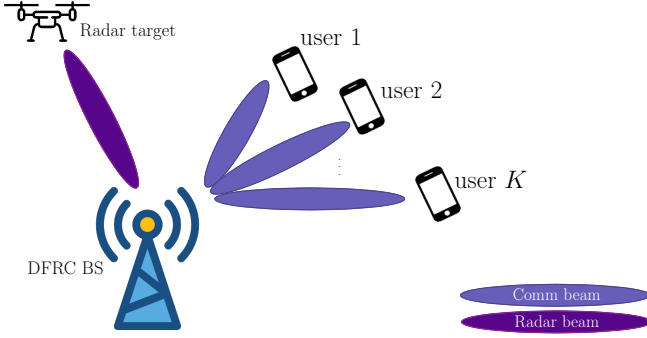


Fig. 1. DFRC scenario including a DFRC base station, an intended target and K communication users.

II. SYSTEM MODEL

Let us consider a dual-functional radar communication (DFRC) system comprised of a target of interest, K single-antenna communication users, and a DFRC base station. The base station is equipped with an antenna array composed of N elements and the array response of a signal arriving at direction θ is denoted as $\mathbf{a}(\theta) \in \mathbb{C}^{N \times 1}$, where its n^{th} entry, $a_n(\theta)$ is the phase shift at the n^{th} antenna due to θ . For example, in a uniform linear array setting, we have that

$$\mathbf{a}(\theta) = [1 \quad e^{j\frac{2\pi}{\lambda}d\sin(\theta)} \quad \dots \quad e^{j\frac{2\pi}{\lambda}(N-1)d\sin(\theta)}]^T, \quad (1)$$

where λ is the wavelength of the signal and d is the inter-element spacing. In Fig. 1, we highlight a use case, where the DFRC base station uses the same signal vector and broadcasts it towards communication users and an intended target of interest. The communication users are assumed to be randomly distributed, whereas the radar beam scan is at a known angle θ_0 from the DFRC base station. Now, let us introduce the communication and radar system models.

A. Communication System Model

A single transmission in the downlink could be expressed as

$$\mathbf{y}_c = \mathbf{H}\mathbf{x} + \mathbf{z}_c, \quad (2)$$

where $\mathbf{y}_c \in \mathbb{C}^{K \times 1}$ is the vector of received signals over all communication users, i.e. the k^{th} entry of \mathbf{y}_c is the signal dedicated towards the k^{th} communication user. The channel matrix is given by $\mathbf{H} = [\mathbf{h}_1 \quad \mathbf{h}_2 \quad \dots \quad \mathbf{h}_K]^T \in \mathbb{C}^{K \times N}$, and is flat Rayleigh type fading, assumed to be constant during one transmission. Furthermore, the transmit signal vector is denoted by \mathbf{x} . Finally, the vector $\mathbf{z}_c \in \mathbb{C}^{K \times 1}$ is background noise, assumed to be white Gaussian i.i.d with zero mean and a multiple of identity covariance matrix as $\mathbf{z}_c \sim \mathcal{N}(0, \sigma_c^2 \mathbf{I}_K)$. Note that the signal \mathbf{x} is used for both communication and sensing tasks, hence the vector \mathbf{x} is also a snapshot of a radar pulse [24]. We further assume that \mathbf{x} is precoded, which is the output of the following linear equation

$$\mathbf{x} = \mathbf{W}\mathbf{s}, \quad (3)$$

where $\mathbf{W} = [\mathbf{w}_1 \quad \mathbf{w}_2 \quad \dots \quad \mathbf{w}_K] \in \mathbb{C}^{N \times K}$ is the beamforming matrix, where its k^{th} column is the beamforming vector

towards the k^{th} user. The vector $\mathbf{s} \in \mathbb{C}^{K \times 1}$ contains the QAM symbols intended for all users. In what follows, the symbols are assumed to be independent from one another with unit variance, i.e. $\mathbb{E}(\mathbf{s}\mathbf{s}^H) = \mathbf{I}_K$.

B. Radar System Model

The radar functionality in the DFRC system should leverage the same transmit signal as the one used for the communication system model, namely \mathbf{x} . In that way, and using only one time slot, the DFRC is capable of achieving dual sensing and communication functionalities. Thanks to the receiving capability of the DFRC base station, and assuming a colocated mono-static MIMO radar setting [25]

$$\mathbf{y}_r = \gamma_0 \mathbf{a}(\theta_0) \mathbf{a}^T(\theta_0) \mathbf{x} + \mathbf{z}_r. \quad (4)$$

We assume that the above reception, sampling and signal processing occur during a time interval termed the coherent processing interval (CPI) [15], which is an interval where sensing parameters (in our case θ_0) remain unchanged. The received signal $\mathbf{y}_r \in \mathbb{C}^{N \times 1}$ is the received radar vector and γ_0 is the complex channel gain of the reflected echo. The angle θ_0 is the angle-of-arrival of the echo. Similar to \mathbf{z}_c , the noise of the radar sub-system is i.i.d Gaussian modeled as $\mathbf{z}_r \sim \mathcal{N}(0, \sigma_r^2 \mathbf{I}_N)$.

C. Key Performance Indicators

To formulate a suitable and robust optimization problem that aims at solving joint sensing and communication problems, it is crucial to define KPIs related to the problem at hand. Based on equations (2) and (3), the SINR of the k^{th} user, under the assumption of independent symbols, could be expressed as

$$\text{SINR}_k = \frac{\mathbb{E}[|\mathbf{h}_k^T \mathbf{w}_k s_k|^2]}{\sum_{\ell=1, \ell \neq k}^K \mathbb{E}[|\mathbf{h}_k^T \mathbf{w}_\ell s_\ell|^2] + \sigma_c^2}. \quad (5)$$

In this case, and according to Shannon-theory, the achievable rate of transmission of the k^{th} communication user could be expressed as

$$R_k = \log_2(1 + \text{SINR}_k). \quad (6)$$

Furthermore, we could write the SINR of the k^{th} communication user as follows

$$\text{SINR}_k = \frac{\mathbf{h}_k^T \mathbf{w}_k \mathbf{w}_k^H \mathbf{h}_k^*}{\sum_{\ell=1, \ell \neq k}^K \mathbf{h}_k^T \mathbf{w}_\ell \mathbf{w}_\ell^H \mathbf{h}_k^* + \sigma_c^2}, \quad (7)$$

where we have assumed unit symbol power, i.e. $\mathbb{E}(|s_k|^2) = 1$. Notice that the SINR of the k^{th} communication user depends only on the k^{th} communication channel. To that extent, we shall impose a practical scenario where the DFRC base station *does not have full channel information knowledge*. Mathematically, the unknown part of the channel is added on top of the known part as follows

$$\text{SINR}_k = \frac{\tilde{\mathbf{h}}_k^T \mathbf{W}_k \tilde{\mathbf{h}}_k^*}{\sum_{\ell=1, \ell \neq k}^K \tilde{\mathbf{h}}_k^T \mathbf{W}_\ell \tilde{\mathbf{h}}_k^* + \sigma_c^2}, \quad (8)$$

where $\mathbf{W}_k = \mathbf{w}_k \mathbf{w}_k^H$. To this extent, the errors $\tilde{\mathbf{h}}_k = \mathbf{h}_k + \Delta \mathbf{h}_k$ are modeled as independent Gaussian random variables with mean \mathbf{h}_k and covariance $\sigma_{\Delta \mathbf{h}_k}^2 \mathbf{I}_N$, i.e. $\tilde{\mathbf{h}}_k \sim \mathcal{N}(\mathbf{h}_k, \sigma_{\Delta \mathbf{h}_k}^2 \mathbf{I}_N)$. Note that vector $\tilde{\mathbf{h}}_k$ can be decomposed into two counter parts: (i) a fixed part that is inferred through channel estimation techniques, such as ZF or LMMSE, applied on a training sequence stage that occurs before the beamforming stage; (ii) a random part $\Delta \mathbf{h}_k \sim \mathcal{N}(\mathbf{0}, \sigma_{\Delta \mathbf{h}_k}^2 \mathbf{I}_N)$, which captures all the uncertainties coming from channel variations and errors on the channel estimation measurements done between the DFRC base station and the k^{th} communication user. This situation is also referred to as imperfect CSI information. Therefore, due to the random nature of the SINR, it makes sense to introduce an outage probability constraint as a QoS indicator of the communication users as

$$\left\{ \Pr(\text{SINR}_k \leq \gamma_k) \leq p_k \right\}_{k=1}^K, \quad (9)$$

where p_k is the well-known outage probability used to ensure a desired SINR level on communication users. Said differently, in average, we can guarantee a minimum SINR level that is γ_k for the k^{th} communication user with a probability of failure equal to p_k .

On the other hand, the radar should maximize the power in the look-direction of the target, i.e. θ_0 . Notice that equation (4) directly implies that the covariance matrix of the radar received echo is given as

$$\begin{aligned} \mathbb{E}[\mathbf{y}_r \mathbf{y}_r^H] &= |\gamma_0|^2 \mathbf{a}(\theta_0) \mathbf{a}^T(\theta_0) \mathbb{E}[\mathbf{x} \mathbf{x}^H] \mathbf{a}^*(\theta_0) \mathbf{a}^H(\theta_0) \\ &\quad + 2 \text{Re} \left[\gamma_0 \mathbf{a}(\theta_0) \mathbf{a}^T(\theta_0) \mathbb{E}[\mathbf{x} \mathbf{z}_r^H] \right] \\ &\quad + \sigma_r^2 \mathbf{I}_N. \end{aligned} \quad (10)$$

Since the noise at the radar sub-system and the signal vector \mathbf{x} are independent, then the second term vanishes. Focusing on the term of interest, the power due to the signal of interest could be expressed as the trace of the first term as

$$\begin{aligned} P(\theta_0) &= \text{Tr} \left(|\gamma_0|^2 \mathbf{a}(\theta_0) \mathbf{a}^T(\theta_0) \mathbf{W} \mathbf{W}^H \mathbf{a}^*(\theta_0) \mathbf{a}^H(\theta_0) \right) \\ &\propto \sum_{k=1}^K \mathbf{a}^T(\theta_0) \mathbf{W}_k \mathbf{a}^*(\theta_0), \end{aligned} \quad (11)$$

where we have used $\mathbb{E}[\mathbf{x} \mathbf{x}^H] = \mathbf{W} \mathbf{W}^H$ and $\|\mathbf{a}(\theta)\|^2$ is a constant. The radar sub-system would then aim at maximizing the power in the look-direction, i.e. $P(\theta_0)$. In array processing terms, $P(\theta)$ is the output of a conventional Bartlett beamformer of a signal arriving at angle θ , with covariance $\mathbf{W} \mathbf{W}^H$.

III. BEAMFORMING DESIGN UNDER IMPERFECT CSI

In a joint sensing and communication approach, the goal is to ideally maximize both radar and communication performances by using the same waveform \mathbf{x} . Alternatively, we can cast the problem as a beamforming design one, where the goal of the DFRC base station is to find the best beamforming matrix that would jointly optimize communication and radar performances.

A. Problem formulation

We start by formulating a suitable joint sensing and communication problem, where the main cost function aims at maximizing the output of a Bartlett beamformer subject to a series of QoS constraint of all communication users involved in the system, that is

$$(\mathcal{P}_1) : \begin{cases} \max_{\{\mathbf{w}_k\}} & P(\theta_0) \\ \text{s.t.} & \Pr(\text{SINR}_k \leq \gamma_k) \leq p_k, \quad \forall k \\ & \sum_{k=1}^K \text{Tr}(\mathbf{W}_k) \leq 1, \\ & \mathbf{W}_k = \mathbf{w}_k \mathbf{w}_k^H, \quad \forall k, \end{cases} \quad (12)$$

where the $\sum_{k=1}^K \text{Tr}(\mathbf{W}_k) \leq 1$ is to reflect the available power budget³. Note that (\mathcal{P}_1) is non-convex due to all the probabilistic constraints involved within the problem. One way of proceeding with the above problem is to derive the exact distribution function associated with the random variable SINR_k , however the closed-form expression of the distribution function leads to a highly non-linear problem. To this end, we shall follow a series of relaxations to arrive at a tractable one.

B. Semi-definite reformulation

We start by re-expressing (\mathcal{P}_1) as follows

$$(\mathcal{P}_1) : \begin{cases} \max_{\{\mathbf{w}_k\}} & P(\theta_0) \\ \text{s.t.} & \Pr\left(\frac{\frac{1}{\gamma_k} \tilde{\mathbf{h}}_k^T \mathbf{W}_k \tilde{\mathbf{h}}_k^*}{\sum_{\ell=1, \ell \neq k}^K \tilde{\mathbf{h}}_k^T \mathbf{W}_\ell \tilde{\mathbf{h}}_k^* + \sigma_c^2} \leq 1\right) \leq p_k, \quad \forall k \\ & \sum_{k=1}^K \text{Tr}(\mathbf{W}_k) \leq 1, \\ & \mathbf{W}_k = \mathbf{w}_k \mathbf{w}_k^H, \quad \forall k. \end{cases} \quad (13)$$

Through straightforward manipulations, one can show that the contribution of the ℓ^{th} beamformer on the k^{th} communication channel could be expressed as

$$\tilde{\mathbf{h}}_k^T \mathbf{W}_\ell \tilde{\mathbf{h}}_k^* = \mathbf{h}_k^T \mathbf{W}_\ell \mathbf{h}_k^* + \Delta \mathbf{h}_k^T \mathbf{W}_\ell \Delta \mathbf{h}_k^* + 2 \text{Re}(\Delta \mathbf{h}_k^T \mathbf{W}_\ell \mathbf{h}_k^*). \quad (14)$$

Using equation (14) in (\mathcal{P}_1) appearing in equation (13), we get

$$\begin{cases} \max_{\{\mathbf{w}_k\}} & P(\theta_0) \\ \text{s.t.} & \Pr\left(\Delta \mathbf{h}_k^T \bar{\mathbf{W}}_k \Delta \mathbf{h}_k^* + 2 \text{Re}(\Delta \mathbf{h}_k^T \bar{\mathbf{W}}_k \mathbf{h}_k^*) \leq \sigma_c^2\right) \leq p_k \\ & \sum_{k=1}^K \text{Tr}(\mathbf{W}_k) \leq 1, \\ & \mathbf{W}_k = \mathbf{w}_k \mathbf{w}_k^H, \quad \forall k \\ & \sigma_c^2 = \sigma_c^2 - \mathbf{h}_k^T \bar{\mathbf{W}}_k \mathbf{h}_k^*, \quad \forall k, \end{cases} \quad (15)$$

where $\bar{\mathbf{W}}_k = \frac{1}{\gamma_k} \mathbf{W}_k - \sum_{\ell=1, \ell \neq k}^K \mathbf{W}_\ell$. Notice now that we have moved all random quantities in the probability to the left-hand side of the inequality within the probability event.

³Indeed, one could easily replace the 1 by a desired power budget, say P_0 .

To standardize the gaussian vector $\Delta \mathbf{h}_k$, we shall introduce normalization factors as follows,

$$\left\{ \begin{array}{l} \max_{\{\mathbf{w}_k\}} P(\theta_0) \\ \text{s.t.} \quad \Pr(\mathbf{z}_k^H \mathbf{A}_k \mathbf{z}_k + 2 \operatorname{Re}(\mathbf{z}_k^H \mathbf{b}_k) \leq \sigma_k^2) \leq p_k \\ \sum_{k=1}^K \operatorname{Tr}(\mathbf{W}_k) \leq 1, \\ \mathbf{W}_k = \mathbf{w}_k \mathbf{w}_k^H, \quad \forall k \\ \sigma_k^2 = \sigma_c^2 - \mathbf{h}_k^T \bar{\mathbf{W}}_k \mathbf{h}_k^*, \quad \forall k, \end{array} \right. \quad (16)$$

where $\mathbf{z}_k = \frac{1}{\sigma_{\Delta \mathbf{h}_k}} \Delta \mathbf{h}_k^*$, $\mathbf{A}_k = \sigma_{\Delta \mathbf{h}_k}^2 \bar{\mathbf{W}}_k$ and $\mathbf{b}_k = \sigma_{\Delta \mathbf{h}_k} \bar{\mathbf{W}}_k \mathbf{h}_k^*$, where $\mathbf{z}_k \sim \mathcal{N}(\mathbf{0}, \mathbf{I}_N)$. Now, making use of *Bernstien-type inequality* for quadratic-type Gaussian processes [22], we can say that for any $\epsilon_k \geq 0$, we have the following

$$\Pr(\mathbf{z}_k^H \mathbf{A}_k \mathbf{z}_k + 2 \operatorname{Re}(\mathbf{z}_k^H \mathbf{b}_k) \leq U_k) \leq \exp(-\epsilon_k), \quad (17)$$

where $U_k = \operatorname{Tr}(\mathbf{A}_k) - \sqrt{2\epsilon_k} \sqrt{\|\operatorname{vec}(\mathbf{A}_k)\|^2 + 2\|\mathbf{b}_k\|^2} - \epsilon_k \lambda_k^-$, where $\lambda_k^- = \max(\lambda_{\max}(-\mathbf{A}_k), 0)$. This is fulfilled by first adjusting $\epsilon_k = -\log(p_k)$ so as to guarantee the same outage probability level as in (\mathcal{P}_1) and upper-bounding σ_k^2 by U_k , we can formulate an equivalent problem

$$(\mathcal{P}_2) : \left\{ \begin{array}{l} \max_{\{\mathbf{w}_k\}} P(\theta_0) \\ \text{s.t.} \quad \sigma_k^2 \leq U_k \\ \sigma_k^2 = \sigma_c^2 - \mathbf{h}_k^T \bar{\mathbf{W}}_k \mathbf{h}_k^*, \quad \forall k \\ \sum_{k=1}^K \operatorname{Tr}(\mathbf{W}_k) \leq 1, \\ \mathbf{W}_k = \mathbf{w}_k \mathbf{w}_k^H, \quad \forall k \\ U_k = \operatorname{Tr}(\mathbf{A}_k) - \sqrt{2\epsilon_k} c_k - \epsilon_k \lambda_k^-, \quad \forall k \\ c_k = \sqrt{\|\operatorname{vec}(\mathbf{A}_k)\|^2 + 2\|\mathbf{b}_k\|^2}, \quad \forall k. \end{array} \right. \quad (18)$$

Notice that problem (\mathcal{P}_2) does not contain a probability event within its constraint. Furthermore, we replace the quadratic constraint $\mathbf{W}_k = \mathbf{w}_k \mathbf{w}_k^H$ with an equivalent one as follows

$$(\mathcal{P}_2) : \left\{ \begin{array}{l} \max_{\{\mathbf{W}_k\}} P(\theta_0) \\ \text{s.t.} \quad \sigma_k^2 \leq U_k \\ \sigma_k^2 = \sigma_c^2 - \mathbf{h}_k^T \bar{\mathbf{W}}_k \mathbf{h}_k^*, \quad \forall k \\ \mathbf{W}_k \succeq \mathbf{0}, \quad \operatorname{rank}(\mathbf{W}_k) = 1, \quad \forall k \\ \sum_{k=1}^K \operatorname{Tr}(\mathbf{W}_k) \leq 1, \\ U_k = \operatorname{Tr}(\mathbf{A}_k) - \sqrt{2\epsilon_k} c_k - \epsilon_k \lambda_k^-, \quad \forall k \\ c_k = \sqrt{\|\operatorname{vec}(\mathbf{A}_k)\|^2 + 2\|\mathbf{b}_k\|^2}, \quad \forall k. \end{array} \right. \quad (19)$$

Next, we introduce K non-negative slack variables, $\nu_1 \dots \nu_K$, where ν_k aims at upper bounding the maximum eigenvalue of $-\mathbf{A}_k$ as

$$\nu_k \mathbf{I}_N \succeq \lambda_k^- \mathbf{I}_N \succeq -\mathbf{A}_k. \quad (20)$$

Introducing the inequality in equation (20) to problem (\mathcal{P}_2)

$$(\mathcal{P}_3) : \left\{ \begin{array}{l} \max_{\{\mathbf{W}_k, \nu_k, \mu_k\}} P(\theta_0) \\ \text{s.t.} \quad \sigma_k^2 \leq U_k \\ \sigma_k^2 = \sigma_c^2 - \mathbf{h}_k^T \bar{\mathbf{W}}_k \mathbf{h}_k^*, \quad \forall k \\ \nu_k \mathbf{I}_N \succeq -\mathbf{A}_k, \quad \forall k \\ \mathbf{W}_k \succeq \mathbf{0}, \quad \operatorname{rank}(\mathbf{W}_k) = 1, \quad \forall k \\ \sum_{k=1}^K \operatorname{Tr}(\mathbf{W}_k) \leq 1, \\ L_k = \operatorname{Tr}(\mathbf{A}_k) - \sqrt{2\epsilon_k} c_k - \epsilon_k \nu_k, \quad \forall k \\ U_k = \operatorname{Tr}(\mathbf{A}_k) - \sqrt{2\epsilon_k} c_k - \epsilon_k \lambda_k^-, \quad \forall k \\ L_k \leq U_k, \quad \forall k \\ c_k = \sqrt{\|\operatorname{vec}(\mathbf{A}_k)\|^2 + 2\|\mathbf{b}_k\|^2}, \quad \forall k \\ \nu_k \geq 0, \quad \forall k. \end{array} \right. \quad (21)$$

Now to resolve constraint $c_k = \sqrt{\|\operatorname{vec}(\mathbf{A}_k)\|^2 + 2\|\mathbf{b}_k\|^2}$, we will introduce K additional non-negative slack variables, $\mu_1 \dots \mu_K$ in the form of second-order cone (SOC) constraints as follows for all k

$$\mu_k \geq \sqrt{\|\operatorname{vec}(\mathbf{A}_k)\|^2 + 2\|\mathbf{b}_k\|^2}, \quad (22)$$

which further relaxes (\mathcal{P}_3) as

$$(\mathcal{P}_4) : \left\{ \begin{array}{l} \max_{\{\mathbf{W}_k, \nu_k, \mu_k\}} P(\theta_0) \\ \text{s.t.} \quad \sigma_k^2 \leq U_k \\ \sigma_k^2 = \sigma_c^2 - \mathbf{h}_k^T \bar{\mathbf{W}}_k \mathbf{h}_k^*, \quad \forall k \\ \nu_k \mathbf{I}_N \succeq -\mathbf{A}_k, \quad \forall k \\ \mathbf{W}_k \succeq \mathbf{0}, \quad \operatorname{rank}(\mathbf{W}_k) = 1, \quad \forall k \\ \sum_{k=1}^K \operatorname{Tr}(\mathbf{W}_k) \leq 1, \\ L_k = \operatorname{Tr}(\mathbf{A}_k) - \sqrt{2\epsilon_k} \mu_k - \epsilon_k \nu_k, \quad \forall k \\ U_k = \operatorname{Tr}(\mathbf{A}_k) - \sqrt{2\epsilon_k} c_k - \epsilon_k \lambda_k^-, \quad \forall k \\ L_k \leq U_k, \quad \forall k \\ c_k = \sqrt{\|\operatorname{vec}(\mathbf{A}_k)\|^2 + 2\|\mathbf{b}_k\|^2}, \quad \forall k \\ \mu_k \geq c_k, \nu_k \geq 0, \quad \forall k \end{array} \right. \quad (23)$$

The SOC constraint in equation (22) could be re-written under a Schur complement type expression, viz.

$$\mu_k \mathbf{I}_{N+N^2} - \begin{bmatrix} \sqrt{2} \mathbf{b}_k \\ \operatorname{vec}(\mathbf{A}_k) \end{bmatrix} \mu_k^{-1} \begin{bmatrix} \sqrt{2} \mathbf{b}_k \\ \operatorname{vec}(\mathbf{A}_k) \end{bmatrix}^H \succeq \mathbf{0}, \quad (24)$$

which is also equivalent to

$$\mathbf{Q}_k \triangleq \left[\begin{array}{c|c} \mu_k & \sqrt{2} \mathbf{b}_k^H \operatorname{vec}(\mathbf{A}_k)^H \\ \hline \sqrt{2} \mathbf{b}_k & \mu_k \mathbf{I}_{N+N^2} \end{array} \right] \succeq \mathbf{0}, \quad \forall k. \quad (25)$$

Injecting the above inequality within problem (\mathcal{P}_4) we get

$$(\mathcal{P}_5) : \left\{ \begin{array}{l} \max_{\left\{ \begin{array}{l} \mathbf{W}_k \\ \nu_k \\ \mu_k \end{array} \right\}} P(\theta_0) \\ \text{s.t.} \quad \sigma_k^2 \leq U_k \\ \sigma_k^2 = \sigma_c^2 - \mathbf{h}_k^T \bar{\mathbf{W}}_k \mathbf{h}_k^*, \quad \forall k \\ \nu_k \mathbf{I}_N \succeq -\mathbf{A}_k, \quad \forall k \\ \mathbf{W}_k \succeq \mathbf{0}, \quad \text{rank}(\mathbf{W}_k) = 1, \quad \forall k \\ \sum_{k=1}^K \text{Tr}(\mathbf{W}_k) \leq 1, \\ L_k = \text{Tr}(\mathbf{A}_k) - \sqrt{2\epsilon_k} \mu_k - \epsilon_k \nu_k, \quad \forall k \\ U_k = \text{Tr}(\mathbf{A}_k) - \sqrt{2\epsilon_k} c_k - \epsilon_k \lambda_k^-, \quad \forall k \\ L_k \leq U_k, \quad \forall k \\ \mathbf{Q}_k \succeq \mathbf{0}, \nu_k \geq 0, \quad \forall k. \end{array} \right. \quad (26)$$

Notice that the constraint $L_k \leq U_k$ is now a redundant constraint, due to the ones added from equations (20) and (25). Therefore, we can eliminate $L_k \leq U_k$. Also, in order to completely remove the constraint $U_k = \text{Tr}(\mathbf{A}_k) - \sqrt{2\epsilon_k} c_k - \epsilon_k \lambda_k^-$, a reasonable modification would be to replace $\sigma_k^2 \leq U_k$ by $\sigma_k^2 \leq L_k$, since the latter guarantees the former.

$$(\mathcal{P}_6) : \left\{ \begin{array}{l} \max_{\left\{ \begin{array}{l} \mathbf{W}_k \\ \nu_k \\ \mu_k \end{array} \right\}} P(\theta_0) \\ \text{s.t.} \quad \sigma_k^2 \leq \text{Tr}(\mathbf{A}_k) - \sqrt{2\epsilon_k} \mu_k - \epsilon_k \nu_k \\ \sigma_k^2 = \sigma_c^2 - \mathbf{h}_k^T \bar{\mathbf{W}}_k \mathbf{h}_k^*, \quad \forall k \\ \nu_k \mathbf{I}_N \succeq -\mathbf{A}_k, \quad \forall k \\ \mathbf{W}_k \succeq \mathbf{0}, \quad \text{rank}(\mathbf{W}_k) = 1, \quad \forall k \\ \sum_{k=1}^K \text{Tr}(\mathbf{W}_k) \leq 1, \\ \mathbf{Q}_k \succeq \mathbf{0}, \nu_k \geq 0, \quad \forall k. \end{array} \right. \quad (27)$$

The problem in (\mathcal{P}_6) is still non-convex due to the rank-1 constraint. A classical remedy to convexify the problem is to drop the rank-1 constraint, which finally leads to problem (\mathcal{P}_7) as follows

$$(\mathcal{P}_7) : \left\{ \begin{array}{l} \max_{\left\{ \begin{array}{l} \mathbf{W}_k \\ \nu_k \\ \mu_k \end{array} \right\}} P(\theta_0) \\ \text{s.t.} \quad \sigma_k^2 \leq \text{Tr}(\mathbf{A}_k) - \sqrt{2\epsilon_k} \mu_k - \epsilon_k \nu_k \\ \sigma_k^2 = \sigma_c^2 - \mathbf{h}_k^T \bar{\mathbf{W}}_k \mathbf{h}_k^*, \quad \forall k \\ \nu_k \mathbf{I}_N \succeq -\mathbf{A}_k, \quad \forall k \\ \mathbf{W}_k \succeq \mathbf{0}, \quad \forall k \\ \sum_{k=1}^K \text{Tr}(\mathbf{W}_k) \leq 1, \\ \mathbf{Q}_k \succeq \mathbf{0}, \nu_k \geq 0, \quad \forall k. \end{array} \right. \quad (28)$$

Finally, we now have a convex optimization problem at our disposal, that could be easily solved using any convex optimization solver, such as the CVX toolbox [32].

C. Rank-one beamforming

In practical PHY layers, beamforming should take place through rank-one solutions, i.e. vectors of the form

$\mathbf{w}_k \mathbf{w}_k^H = \mathbf{W}_k$. Otherwise, sub-optimal post-processing methods are needed to provide rank-one approximations of \mathbf{W}_k . In the literature, the most common approximations are Gaussian randomization [19], [26] and principle component analysis [27] on \mathbf{W}_k .

However, in some particular scenarios, the rank-one relaxation does not introduce any sort of suboptimality due to the special structure of the problem. For example, the relaxation in [28] has been proven to be exact and thus always gives rank-1 optimal solution in the context of collaborative relay beamforming. Another instance appears in [29] for joint sensing and communication design with low-PAPR waveform constraints. To this extent, we introduce the following theorem:

Theorem 1 (Rank-one Optimality): *Consider the convex optimization problem (\mathcal{P}_7) given in equation (28). Then, for all $k = 1 \dots K$, the solution of (\mathcal{P}_7) satisfies*

$$\text{rank}(\mathbf{W}_k^{\text{opt}}) = 1. \quad (29)$$

Proof: See Appendix A.

Now, that we have a guarantee of rank-one solutions, an eigenvalue decomposition per $\mathbf{W}_k^{\text{opt}}$ is done to recover $\mathbf{w}_k^{\text{opt}}$.

D. Single-user closed-form solutions

In the single user case, we bring special insights to the joint sensing and communication optimization problem in hand. To this end, and for $K = 1$, the problem appearing in (\mathcal{P}_6) boils down to

$$(\mathcal{P}_6^{\text{SU}}) : \left\{ \begin{array}{l} \max_{\{\mathbf{w}, \nu, \mu\}} |\mathbf{a}^T(\theta_0) \mathbf{w}|^2 \\ \text{s.t.} \quad \sigma_c^2 - \frac{1}{\gamma} |\mathbf{h}^T \mathbf{w}|^2 \leq \frac{\sigma_\Delta^2}{\gamma} \|\mathbf{w}\|^2 - \sqrt{2\epsilon} \mu - \epsilon \nu \\ \nu \mathbf{I}_N \succeq -\frac{\sigma_\Delta^2}{\gamma} \mathbf{w} \mathbf{w}^H \\ \|\mathbf{w}\|^2 \leq 1 \\ \mu \geq \sqrt{\|\text{vec}(\mathbf{A})\|^2 + 2\|\mathbf{b}\|^2} \\ \nu \geq 0, \end{array} \right. \quad (30)$$

where we have denoted, for sake of simplicity, the single user channel as $\mathbf{h} \triangleq \mathbf{h}_1$, the SINR threshold as $\gamma \triangleq \gamma_1$, the channel error variance as $\sigma_\Delta \triangleq \sigma_\Delta^2 \mathbf{h}_1$, the slack variables $\nu_1 \triangleq \nu$, $\mu_1 \triangleq \mu$, the $\epsilon_1 \triangleq \epsilon$ and finally the beamforming vector $\mathbf{w}_1 \triangleq \mathbf{w}$. Note that the semi-definite constraint $\nu \mathbf{I}_N \succeq -\frac{\sigma_\Delta^2}{\gamma} \mathbf{w} \mathbf{w}^H$ along with the non-negativity constraint on ν defines the region $\nu \geq 0 \geq -\frac{\sigma_\Delta^2}{\gamma} \|\mathbf{w}\|^2$. Using this region and the identity $\|\text{vec}(\mathbf{A})\|^2 = \text{Tr}(\mathbf{A}^H \mathbf{A}) = \frac{\sigma_\Delta^4}{\gamma^2} \|\mathbf{w}\|^4$ and $\|\mathbf{b}\|^2 = \frac{\sigma_\Delta^2}{\gamma^2} |\mathbf{h}^T \mathbf{w}|^2 \|\mathbf{w}\|^2$

$$(\mathcal{P}_6^{\text{SU}}) : \left\{ \begin{array}{l} \max_{\mathbf{w}} |\mathbf{a}^T(\theta_0) \mathbf{w}|^2 \\ \text{s.t.} \quad \gamma \sigma_c^2 - f_\epsilon(\mathbf{w}) \|\mathbf{w}\|^2 \leq |\mathbf{h}^T \mathbf{w}|^2 \\ \|\mathbf{w}\|^2 \leq 1, \end{array} \right. \quad (31)$$

where $f_\epsilon(\mathbf{w}) = \sigma_\Delta^2 - \sqrt{2\epsilon} \sigma_\Delta \sqrt{\sigma_\Delta^2 + 2 \frac{|\mathbf{h}^T \mathbf{w}|^2}{\|\mathbf{w}\|^2}}$. We now present the next theorem:

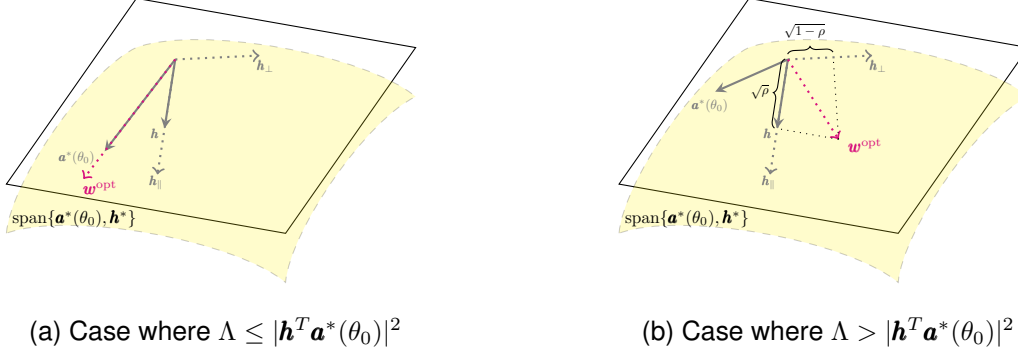


Fig. 2. Graphical interpretation of the DFRC beamforming weight vector, as a function of steering vector and mean channel response.

Theorem 2 (Single-User BFin in Closed-Form, $\epsilon \rightarrow 0$): Let $K = 1$, the optimal solution to problem (\mathcal{P}_6^{SU}) when $\epsilon = 0$, is given as follows

$$\mathbf{w}^{\text{opt}} = \begin{cases} \frac{\mathbf{a}^*(\theta_0)}{\|\mathbf{a}^*(\theta_0)\|}, & \text{if } N(\gamma\sigma_c^2 - \sigma_\Delta^2) \leq |\mathbf{h}^T \mathbf{a}^*(\theta_0)|^2 \\ \sqrt{\rho} \frac{\mathbf{h}_{\parallel}^H \mathbf{a}^*(\theta_0)}{\|\mathbf{h}_{\parallel}^H \mathbf{a}^*(\theta_0)\|} \mathbf{h}_{\parallel} + \sqrt{1-\rho} \frac{\mathbf{h}_{\perp}^H \mathbf{a}^*(\theta_0)}{\|\mathbf{h}_{\perp}^H \mathbf{a}^*(\theta_0)\|} \mathbf{h}_{\perp}, & \text{else} \end{cases} \quad (32)$$

given the following feasibility condition

$$0 \leq \rho \triangleq \frac{\gamma\sigma_c^2 - \sigma_\Delta^2}{\|\mathbf{h}\|^2} \leq 1. \quad (33)$$

Proof: See Appendix B.

The closed-form solution in equation (32) brings many useful insights. When the channel \mathbf{h} and the steering vector towards the look direction, i.e. $\mathbf{a}(\theta_0)$, are highly correlated, then the solution is the Bartlett beamformer. In other words, the efforts spent on maximizing the SINR are obtained via the radar metric. Note that the threshold that determines the degree of correlation between the channel and the steering vector in the look direction is $N(\gamma\sigma_c^2 - \sigma_\Delta^2)$. From here, we can see that the given γ has an impact on deciding the radar-communication tradeoff. With increasing γ , we are enforcing a strong correlation between the channel and the steering vectors to return a full radar solution. On the other hand, if low correlation exists, then both the channel and the steering vectors contribute to the solution. Specifically, and from a communication perspective, an extreme case is realized upon adjusting γ so that $\rho = 1$, where the optimal beamforming vector is now a matched filter solution. Interestingly, the feasibility of the problem is expressed as the maximum achievable average-SINR defined in equation (65). We can further generalize **Theorem 2** as follows

Theorem 3 (Single-User BFin in Closed-Form): Let $K = 1$, the optimal solution to problem (\mathcal{P}_6^{SU}) , is given as follows

$$\mathbf{w}^{\text{opt}} = \begin{cases} \frac{\mathbf{a}^*(\theta_0)}{\|\mathbf{a}^*(\theta_0)\|}, & \text{if } \Lambda \leq |\mathbf{h}^T \mathbf{a}^*(\theta_0)|^2 \\ \sqrt{\rho} \frac{\mathbf{h}_{\parallel}^H \mathbf{a}^*(\theta_0)}{\|\mathbf{h}_{\parallel}^H \mathbf{a}^*(\theta_0)\|} \mathbf{h}_{\parallel} + \sqrt{1-\rho} \frac{\mathbf{h}_{\perp}^H \mathbf{a}^*(\theta_0)}{\|\mathbf{h}_{\perp}^H \mathbf{a}^*(\theta_0)\|} \mathbf{h}_{\perp}, & \text{else} \end{cases} \quad (34)$$

where $\Lambda = N(\gamma\sigma_c^2 - \sigma_\Delta^2 + \sqrt{2\epsilon}\sigma_\Delta \sqrt{\sigma_\Delta^2 + 2\frac{|\mathbf{h}^T \mathbf{a}^*(\theta_0)|^2}{N}})$ and $\sqrt{\rho}$ is a root of the following equation in the interval $[0, 1]$

$$g(x) = x^2 \|\mathbf{h}\|^2 - (\gamma\sigma_c^2 - \sigma_\Delta^2) - \sigma_\Delta \sqrt{2\epsilon} \sqrt{\sigma_\Delta^2 + x^2 \|\mathbf{h}\|^2}. \quad (35)$$

The proof of the above theorem follows similar steps as in the proof found in Appendix B. Note that when $\epsilon \rightarrow 0$, the expressions found in **Theorem 3** coincide with that in **Theorem 2**.

Note that **Theorem 3** reveals the impact of outage probability rate p , or equivalently ϵ . In particular, the more we restrict a tighter outage SINR failure, the larger Λ is. To summarize, both γ and p have a direct influence on the radar-communication tradeoffs as Λ scales as $\mathcal{O}(\gamma)$ and $\mathcal{O}(\epsilon^{\frac{1}{2}})$. To illustrate this, a graphical interpretation is given in Fig. 2.

IV. SIMULATION RESULTS

In this section, various simulation results are conducted to illustrate the performance and trade-offs achieved with the proposed beamforming waveform design. Through all simulations, we assume that the channel error variations are equal, namely $\sigma_{\Delta h_1} = \dots = \sigma_{\Delta h_K} = \sigma_\Delta$. Unless otherwise stated, we set $\sigma_\Delta = 0.1$. Likewise, we set all outage parameters per communication user to be the same, i.e. $p_1 = \dots = p_K = p$ and $\gamma_1 = \dots = \gamma_K = \gamma$. Simulation results are realized through Monte Carlo averaging, where each point generated is averaged over 10^3 Monte Carlo trials. The channels \mathbf{h}_k and the imperfect CSI $\Delta \mathbf{h}_k$ are drawn from a complex Gaussian distribution with zero mean. We have also used CVX as a solver [32] to generate the beamforming solutions of problem (\mathcal{P}_7) . A uniform linear array spaced at half a wavelength apart has been considered here.

A. Influence of γ on the achievable rate

We start the simulation section by studying the total achievable rate, when γ is the varying factor, in Fig. 3. We set $p = 0.1$ and $\theta_0 = 30^\circ$. In terms of rate achievability, and as expected, we observe a rising trend with increasing γ or increasing number of users. For sake of argument, let us first focus on the case of $K = 2$, we can see that at $\gamma = 1$ dB, the achieved rate is very close to the threshold, i.e. $2 \log_2(1 + \gamma) \simeq 2.17$ bits/sec/Hz. On the other hand, notice that at $\gamma = 2$ dB, we are expecting a total rate of at least 2.35 bits/sec/Hz, however, the actual achieved rate is 5.39 bits/sec/Hz. Even though users are subject to imperfect CSI, we observe a rising trend between the total achievable

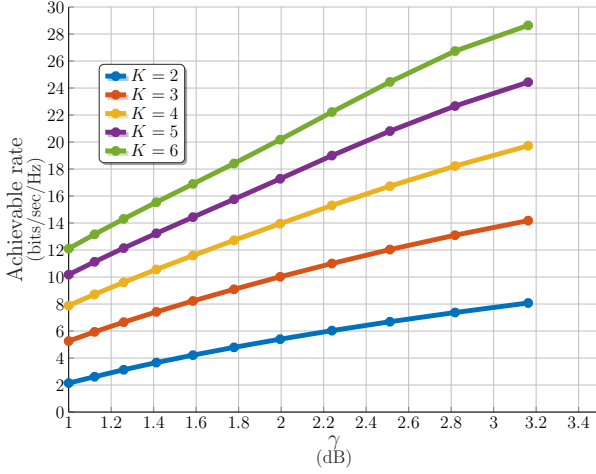


Fig. 3. Achievable rates as a function of γ for different values of K at $N = 10$ antennas and $p = 0.1$.

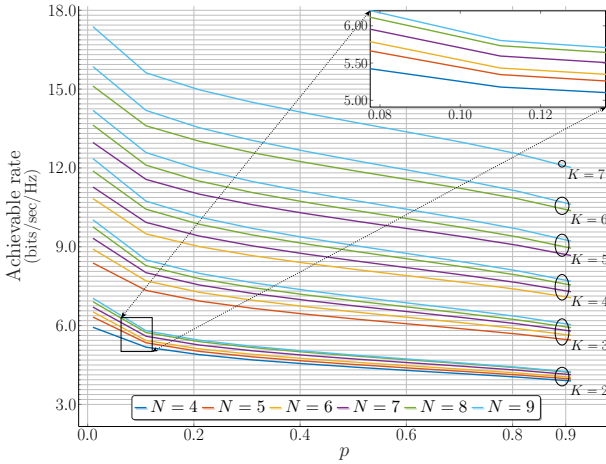


Fig. 4. Achievable rates as a function of p for different values of N and K .

rate and the one being probed for, with increasing number of users, as well. As we will see in simulations below, this trend could be controlled through the outage probability p .

B. Influence of p on the achievable rate

In the simulations shown in Fig. 4, we aim at studying the impact of p on the total achievable rate with different number of transmit antennas and communication users. It is clear that increasing p leads to a degradation in the total achievable rate. In particular, a breakout region is observed around $p = 0.1$, where beyond this value, a stable slope contributes in the decrease of the total achievable rate. On another note, the degrees of freedom (DoF) available accounts for additional improvement in terms of SINR, due to additional nulling of the interference terms; therefore, an increase in the total achievable rate. As an example, for the case of $K = 2$, doubling the number of antennas contribute to an increase

of roughly 0.3 bits/sec/Hz, whereas the same rate increase could be attained by adding only 1 antenna, when $K = 5$.

C. Feasibility rate

Another aspect we intend to shed light on is the feasibility rate. A solution is deemed infeasible when either one of the constraints of problem \mathcal{P}_7 is violated or when a solution is not available; therefore, a reasonable way to simulate the feasibility rate is through

$$\text{feasibility rate} = \frac{\# \text{ of feasible solutions}}{\# \text{ of cases}}. \quad (36)$$

Setting the number of transmit antennas to $N = 6$, we aim at concluding some allowable SINR thresholds with different number of communication users. As expected, the larger γ is, the tighter is the feasibility region attained for our joint beamforming design, for any p and K . Nonetheless, another nice interpretation of p is its direct impact on the feasibility region. Said differently, a larger p dilates the feasibility region, while sacrificing lower achievable rate, according to the previous simulations in Fig. 4. For example, for the case of $K = 2$ communication users, our beamforming design is 99% capable of returning a feasible solution for an SINR target of $\gamma = 3.8$ dB. At this feasibility level, one could increase the target by roughly 1.4 dB, just by incrementing the outage rate by 0.1, as depicted in Fig. 5 for $K = 2$. Furthermore, as K increases, it is evident that expected SINR target levels should shrink down, due to the unit power budget constraint. For example, at a feasibility rate of 99%, we see that we can target $\gamma = 1.6$ dB for $K = 3$ users, compared to $\gamma = 1.25$ dB for $K = 4$.

D. ISMR-rate trade-off

So far, we have only addressed the communication performance, without dedicating any attention to radar metrics. To include the impact of radar metrics, we discuss different radar-communication tradeoffs, with emphasis on two well-known radar-communication tradeoffs, namely, the integrated-sidelobe-to-mainlobe-ratio⁴ (ISMR) and the probability of detection. We start with the former.

The ISMR metric measures the energy in the sidelobe relative to the mainlobe and is defined as follows

$$\text{ISMR} = \frac{\int_{\Theta_s} P(\theta) d\theta}{\int_{\Theta_m} P(\theta) d\theta} = \frac{\text{Tr}(\mathbf{W}\mathbf{W}^H \mathbf{A}_s)}{\text{Tr}(\mathbf{W}\mathbf{W}^H \mathbf{A}_m)}, \quad (37)$$

where Θ_m is the mainlobe region and Θ_s is the sidelobe region and $\mathbf{A}_{s/m} = \int_{\Theta_{s/m}} \mathbf{a}(\theta)\mathbf{a}^H(\theta) d\theta$, whose expression for uniform linear arrays is given in [34]. Note that the ISMR computation requires specification of the mainlobe and sidelobe supports. We have specified the mainlobe and sidelobe regions to be $\Theta_m = [\theta_0 \pm \frac{\Delta}{2}]$ and $\Theta_s = [-\frac{\pi}{2}, \theta_0 - \frac{\Delta}{2}] \cup [\theta_0 + \frac{\Delta}{2}, \frac{\pi}{2}]$, where we have set $\Delta = 20^\circ$. Moreover, its

⁴Even though our beamforming design does not explicitly optimize ISMR terms, it does make absolute sense to include this metric in our analysis route. This is due to the fact that our cost function maximizes the output of the Bartlett beamformer in the look direction, θ_0 . Therefore, to measure this mainlobe power, the sidelobe power should be taken as reference.

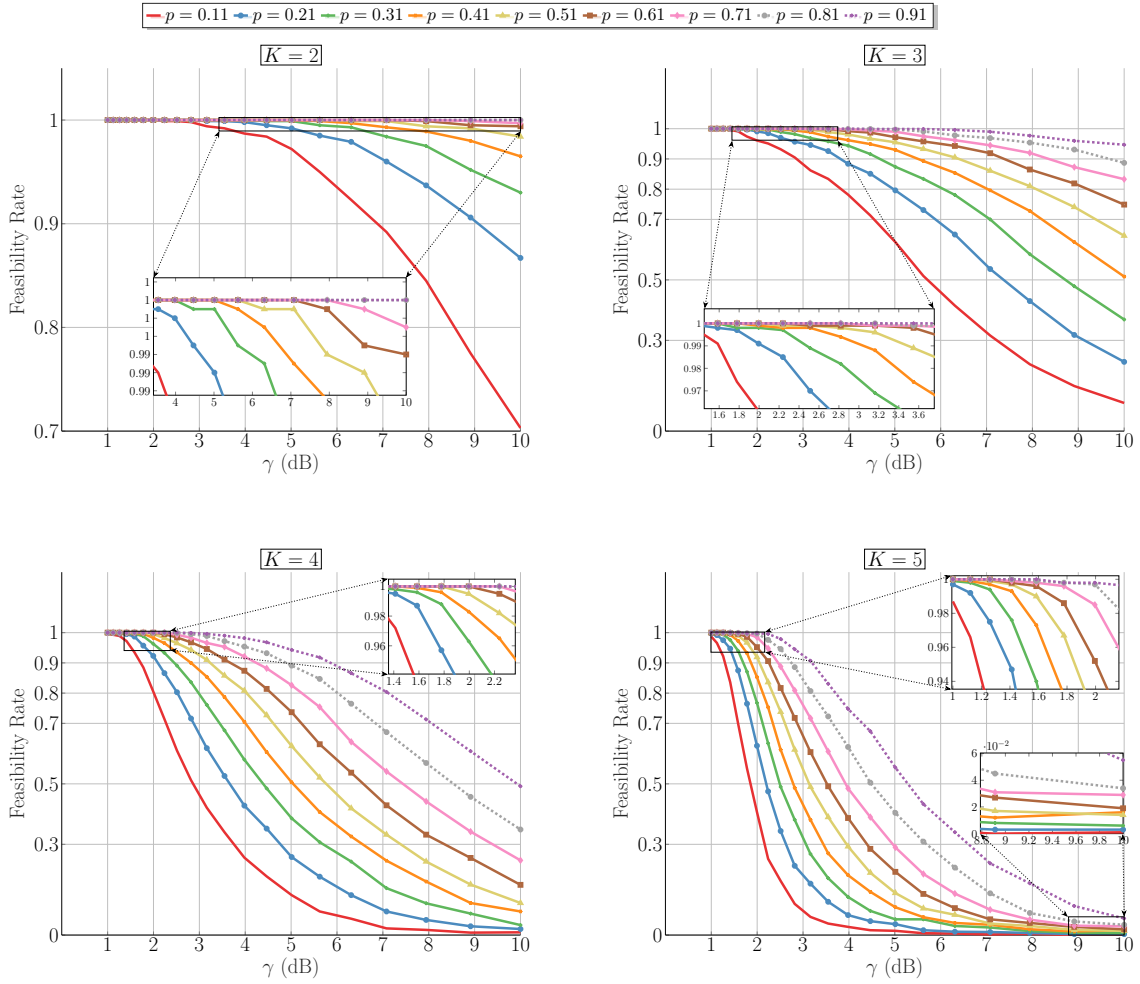


Fig. 5. Feasibility rate behavior with varying γ at $N = 6$ for different number of communication users at a target located at $\theta_0 = 30^\circ$.

inverse, ISMR^{-1} , reports the amount of energy concentrated in the mainlobe relative to that of the sidelobe. According to Fig. 6 and Fig. 7, it is clear that a trade-off between the average communication rate and the radar ISMR^{-1} performance exists. In particular, for a fixed ISMR^{-1} level, the average achievable rate increases with either an increase in γ or a decrease in number of communication users, K . For example, fixing $\text{ISMR}^{-1} = 22$ dB, one could increase the average achievable rate by roughly 0.33 bits/sec/Hz either by increasing γ by a factor of 3 dB, or by operating with 2 less communication users, or by increasing the DoFs available. Therefore, both γ and p have a direct influence on the radar-communication tradeoff.

E. Probability of detection and rate trade-off

Another tradeoff we can study is the probability of detection P_D , vs the average achievable sum rate. We calculate the detection probability following [33] as

$$P_D = 1 - \mathcal{F}_{\chi_2^2(\rho)}\left(\mathcal{F}_{\chi_2^2}^{-1}(1 - P_{\text{FA}})\right) \quad (38)$$

where $\rho = \text{SNR}_r |\mathbf{a}^H(\theta_0) \mathbf{R}_{xx} \mathbf{a}(\theta_0)|^2$. The radar SNR is defined as SNR_r and is fixed to 1 dB. We set $N = 5$ antennas. The probability of false-alarm for radar is $P_{\text{FA}} = 10^{-4}$. To show the superiority of our design, we compare to the beamforming design in [24]. Referring to Fig. 8, it is clear that a trade-off, similar to that in Fig. 7, exists between the detection performance of the radar and the communication rate. In other words, for a fixed P_D , the rate increases with a decrease in number of users. Second, it should be noted that our design presents better tradeoffs in both, probability of detection and average achievable rate, especially when K grows large. For example, with $K = 4$ and an average achievable sum-rate of 4.78 bits/sec/Hz/user, we have that $P_D \simeq 0.65$, when the design in [24] is adopted; compared to $P_D \simeq 0.99$ using the proposed design, herein. This gain could be explained as follows: The design in [24] is a two-step procedure. In the first step, the desired radar-only waveform is obtained through the desired covariance matrix, then in the second step, a weighted optimization problem is formulated that trades off a similarity constraint on the radar waveform and the MUI (Multi-user Interference). This decoupling of problems could introduce

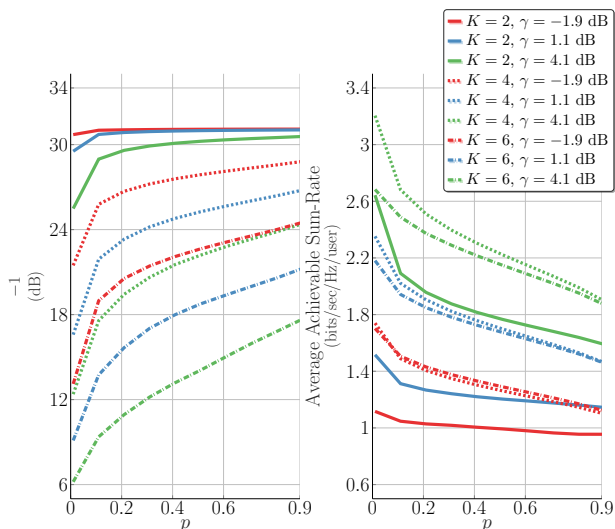


Fig. 6. Behavior of the average achievable sum rate per user and the ISMR for $N = 7$.

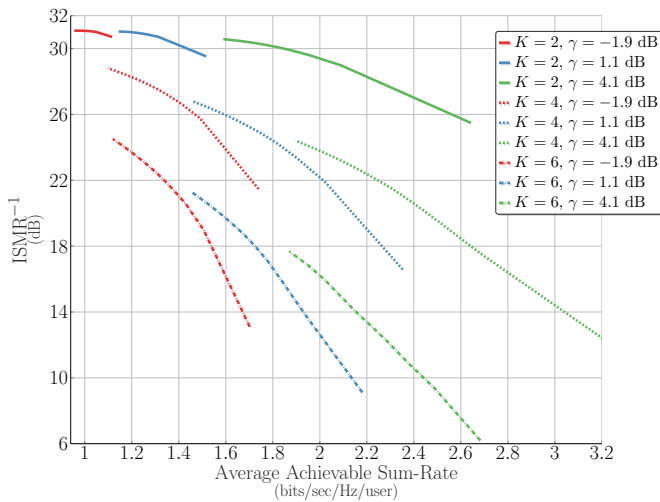


Fig. 7. Trade-off between the average achievable sum rate per user and the beampattern's ISMR for $N = 7$.

some sub-optimality to the joint radar-communication designs. Another aspect is the inherit modeling of random channel behavior in our design. On the other hand, our design cannot account for a desired beampattern, as opposed to that in [24]. In other words, the proposed design does not offer any control over beamwidths, sidelobe rejection ratios, etc. This is due to the fact that we maximize the power in the desired look direction, without explicit indication of the aforementioned radar properties.

F. Beampattern trade-offs

We also study several instances of the resulting beampattern through our design. It can be seen that not only lower sidelobes are achieved by lowering γ , but also a better accuracy in terms of look direction. For example, fixing $N = 10$ with $K = 4$ users, setting the look direction in $\theta_0 = 30^\circ$ as in Fig. 9a, we

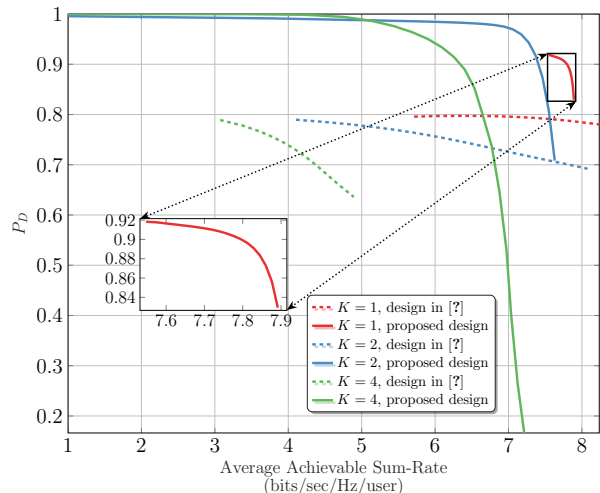


Fig. 8. Trade-off between the average achievable sum rate per user and the radar detection probability for $N = 5$ at receive $\text{SNR}_r = 1$ dB, and $P_{\text{FA}} = 10^{-4}$.

can see that a decrementation of γ by a factor of 3 contributes to a sidelobe decrease of roughly 10 dB and an improvement in the look direction in the order of 0.5° . A similar interpretation could be given in Fig. 9b, where the look-direction has been changed to $\theta_0 = 66^\circ$.

V. CONCLUSION

In this paper, we have proposed an outage-based dual-functional radar-communication beamforming design aware of imperfect CSI, achieving high communication rates and detecting passive targets. To begin with, we have formulated an optimization problem that maximizes the output of the Bartlett beamformer towards the target, under outage signal-to-interference-plus-noise ratio constraints. Under some diligent relaxations, we arrive at a relaxed convex optimization problem, which can be tackled via numerical solvers, such as CVX. In terms of optimality, we prove that the final problem is always guaranteed to generate rank-one beamforming solutions. Furthermore, we derive closed-form solutions of the problem for the single-user case, shed light on several interesting radar-communication trade-offs, and draw attention to gains, in the presence of imperfect CSI, achieved in radar through deliberate loss in communications, and vice-versa. Finally, and via numerical simulations, we show the superiority of the proposed beamforming design, as compared to state-of-the-art radar-communication beamformers.

Future research will be oriented towards joint sensing and communication beamforming and waveform design for multiple targets and imperfect CSI case. Other performance radar and communication metrics could be taken into consideration. Nevertheless, future work will also consider estimation aspects of the radar subproblem and its impact on the communication performance.

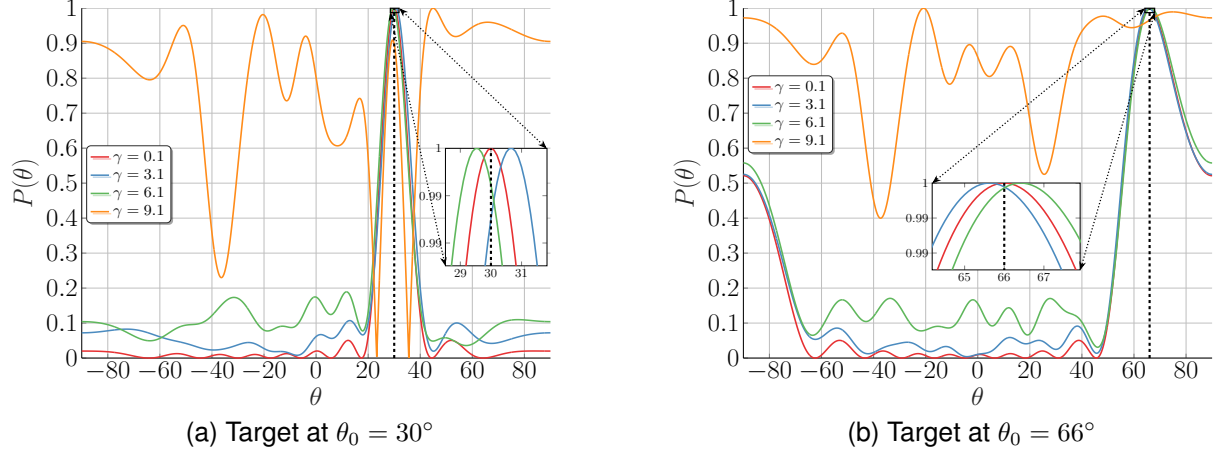


Fig. 9. Resulting radar beampatterns for different values of γ at $N = 10, K = 4$ for different look directions, θ_0 .

APPENDIX A RANK-1 OPTIMALITY

We begin by writing down the Lagrangian function associated with problem (\mathcal{P}_7) , which is

$$\begin{aligned} \mathcal{L}(\mathbf{W}_1 \dots \mathbf{W}_K, \zeta, \mathbf{a}, \boldsymbol{\alpha}, \boldsymbol{\Psi}, \mathbf{Z}) & \\ = \sum_{k=1}^K \text{Tr}(\Phi \mathbf{W}_k) + \sum_{k=1}^K \text{Tr}(\mathbf{Z}_k \mathbf{Q}_k) + \sum_{k=1}^K a_k \nu_k & \\ + \sum_{k=1}^K \alpha_k \left(\text{Tr}(\mathbf{A}_k) - \sqrt{2\epsilon_k} \mu_k - \epsilon_k \nu_k - \sigma_c^2 + \mathbf{h}_k^T \bar{\mathbf{W}}_k \mathbf{h}_k^* \right) & \quad (39) \\ + \sum_{k=1}^K \left(\nu_k \text{Tr}(\boldsymbol{\Psi}_k) + \text{Tr}(\boldsymbol{\Psi}_k \mathbf{A}_k) \right) - \zeta \left(\sum_{k=1}^K \text{Tr}(\mathbf{W}_k) - 1 \right), & \end{aligned}$$

where $\zeta \geq 0$, $\alpha_k \geq 0$, $a_k \geq 0$ and $\boldsymbol{\Psi}_k \succeq \mathbf{0}$, $\mathbf{Z}_k \succeq \mathbf{0}$ are Lagrangian dual variables. Let us define $\Phi = \mathbf{a}(\theta_0) \mathbf{a}^H(\theta_0)$ and let us partition \mathbf{Z}_k in the same way \mathbf{Q}_k is partitioned, namely,

$$\mathbf{Z}_k = \begin{bmatrix} z_k & \boldsymbol{\lambda}_k^H & \mathbf{y}_k^H \\ \boldsymbol{\lambda}_k & \mathbf{\Pi}_k & \\ \mathbf{y}_k & & \end{bmatrix}, \quad (40)$$

and so using trace properties of block matrices, we can write $\text{Tr}(\mathbf{Z}_k \mathbf{Q}_k)$ as a quadratic function in $\sigma_{\Delta \mathbf{h}_k}$ as follows

$$\text{Tr}(\mathbf{Z}_k \mathbf{Q}_k) = \kappa_k + \sqrt{2} \sigma_{\Delta \mathbf{h}_k} \text{Tr}(\bar{\mathbf{W}}_k \boldsymbol{\Upsilon}_k) + \sigma_{\Delta \mathbf{h}_k}^2 \text{Tr}(\bar{\mathbf{W}}_k \mathbf{Y}_k), \quad (41)$$

where $\kappa_k = \mu_k z_k + \mu_k \text{Tr}(\mathbf{\Pi}_k)$ appears due to the diagonal contributions, $\boldsymbol{\Upsilon}_k = \mathbf{h}_k^* \boldsymbol{\lambda}_k^H + \boldsymbol{\lambda}_k \mathbf{h}_k^T$ and $\mathbf{Y}_k = \text{vec}^{-1}(\mathbf{y}_k) + \text{vec}^{-H}(\mathbf{y}_k)$ appear due to the first column/row of \mathbf{Q}_k , \mathbf{Z}_k , viz.

$$\begin{aligned} \mathbf{y}_k^H \text{vec}(\mathbf{A}_k) + \text{vec}^H(\mathbf{A}_k) \mathbf{y}_k & \\ = \text{Tr}(\text{vec}^{-1}(\mathbf{y}_k) \mathbf{A}_k) + \text{Tr}(\text{vec}^{-H}(\mathbf{y}_k) \mathbf{A}_k) & \quad (42) \\ = \text{Tr}(\mathbf{A}_k \mathbf{Y}_k) & \\ = \sigma_{\Delta \mathbf{h}_k}^2 \text{Tr}(\bar{\mathbf{W}}_k \mathbf{Y}_k), & \end{aligned}$$

and

$$\begin{aligned} \boldsymbol{\lambda}_k^H \mathbf{b}_k + \mathbf{b}_k^H \boldsymbol{\lambda}_k & = \sigma_{\Delta \mathbf{h}_k} (\boldsymbol{\lambda}_k^H \bar{\mathbf{W}}_k \mathbf{h}_k^* + \mathbf{h}_k^T \bar{\mathbf{W}}_k \boldsymbol{\lambda}_k) \\ & = \sigma_{\Delta \mathbf{h}_k} \text{Tr}(\bar{\mathbf{W}}_k \boldsymbol{\Upsilon}_k). \end{aligned} \quad (43)$$

Now the Lagrangian function could be expressed as follows

$$\begin{aligned} \mathcal{L}(\mathbf{W}_1 \dots \mathbf{W}_K, \zeta, \mathbf{a}, \boldsymbol{\alpha}, \boldsymbol{\Psi}, \mathbf{Z}) & \\ = \sum_{k=1}^K \text{Tr}(\Phi \mathbf{W}_k) + \sum_{k=1}^K \text{Tr}(\boldsymbol{\Omega}_k \bar{\mathbf{W}}_k) - \zeta \sum_{k=1}^K \text{Tr}(\mathbf{W}_k) & \quad (44) \\ + \sum_{k=1}^K \alpha_k \left(-\sqrt{2\epsilon_k} \mu_k - \epsilon_k \nu_k - \sigma_c^2 \right) & \\ + \sum_{k=1}^K \left(\nu_k \text{Tr}(\boldsymbol{\Psi}_k) + \kappa_k + a_k \nu_k \right) + \zeta, & \end{aligned}$$

where

$$\boldsymbol{\Omega}_k = \sqrt{2} \sigma_{\Delta \mathbf{h}_k} \boldsymbol{\Upsilon}_k + \sigma_{\Delta \mathbf{h}_k}^2 (\mathbf{Y}_k + \boldsymbol{\Psi}_k) + \alpha_k (\sigma_{\Delta \mathbf{h}_k}^2 \mathbf{I} + \mathbf{h}_k^* \mathbf{h}_k^T). \quad (45)$$

Using the expression of $\bar{\mathbf{W}}_k = \frac{1}{\gamma_k} \mathbf{W}_k - \sum_{\ell \neq k} \mathbf{W}_\ell$, we have

$$\begin{aligned} \mathcal{L}(\mathbf{W}_1 \dots \mathbf{W}_K, \zeta, \mathbf{a}, \boldsymbol{\alpha}, \boldsymbol{\Psi}, \mathbf{Z}) & \\ = \sum_{k=1}^K \left(\text{Tr}(\Phi \mathbf{W}_k) + \frac{1}{\gamma_k} \text{Tr}(\boldsymbol{\Omega}_k \mathbf{W}_k) - \text{Tr}(\boldsymbol{\Omega}_{\bar{k}} \mathbf{W}_k) - \zeta \text{Tr}(\mathbf{W}_k) \right) & \quad (46) \\ + \sum_{k=1}^K \alpha_k \left(-\sqrt{2\epsilon_k} \mu_k - \epsilon_k \nu_k - \sigma_c^2 \right) & \\ + \sum_{k=1}^K \left(\nu_k \text{Tr}(\boldsymbol{\Psi}_k) + \kappa_k + a_k \nu_k \right) + \zeta, & \end{aligned}$$

where we have used $\sum_{k=1}^K \sum_{\ell \neq k} \text{Tr}(\boldsymbol{\Omega}_k \mathbf{W}_\ell) = \sum_{k=1}^K \text{Tr}(\boldsymbol{\Omega}_{\bar{k}} \mathbf{W}_k)$ where $\boldsymbol{\Omega}_{\bar{k}} = \sum_{\ell \neq k} \boldsymbol{\Omega}_\ell$. The Lagrange dual function is then defined as follows

$$g(\zeta, \mathbf{a}, \boldsymbol{\alpha}, \boldsymbol{\Psi}, \mathbf{Z}) = \max_{\{\mathbf{W}_k \succeq \mathbf{0}\}} \mathcal{L}(\mathbf{W}_1 \dots \mathbf{W}_K, \zeta, \mathbf{a}, \boldsymbol{\alpha}, \boldsymbol{\Psi}, \mathbf{Z}). \quad (47)$$

But since problem (\mathcal{P}_7) is a convex optimization problem with zero duality gap, we can solve the problem via its dual, namely

$$(\mathcal{D}) : \min_{\substack{\zeta \geq 0 \\ \{a_k, \alpha_k \geq 0\} \\ \{\boldsymbol{\Psi}_k, \mathbf{Z}_k \succeq \mathbf{0}\}}} g(\zeta, \mathbf{a}, \boldsymbol{\alpha}, \boldsymbol{\Psi}, \mathbf{Z}). \quad (48)$$

Let us denote the optimal solution of problem (\mathcal{D}) as $\zeta^{\text{opt}}, \mathbf{a}^{\text{opt}}, \boldsymbol{\alpha}^{\text{opt}}, \boldsymbol{\Psi}^{\text{opt}}, \mathbf{Z}^{\text{opt}}$ then the matrices $\mathbf{W}_1^{\text{opt}} \dots \mathbf{W}_K^{\text{opt}}$ that

maximize $\mathcal{L}(\mathbf{W}_1 \dots \mathbf{W}_K, \zeta^{\text{opt}}, \mathbf{a}^{\text{opt}}, \boldsymbol{\alpha}^{\text{opt}}, \boldsymbol{\Psi}^{\text{opt}}, \mathbf{Z}^{\text{opt}})$ is the optimal solution of (\mathcal{P}_7) , which means we can find the optimal solution $\mathbf{W}_1^{\text{opt}} \dots \mathbf{W}_K^{\text{opt}}$ thru the following problem

$$\max_{\mathbf{W}_k \succeq \mathbf{0}} \text{Tr}(\Phi \mathbf{W}_k) - \text{Tr} \left\{ \left(\zeta^{\text{opt}} \mathbf{I} + \boldsymbol{\Omega}_k^{\text{opt}} - \frac{1}{\gamma_k} \boldsymbol{\Omega}_k^{\text{opt}} \right) \mathbf{W}_k \right\}, \quad (49)$$

where

$$\boldsymbol{\Omega}_k^{\text{opt}} = \sqrt{2} \sigma_{\Delta} \mathbf{h}_k \mathbf{T}_k^{\text{opt}} + \sigma_{\Delta}^2 \mathbf{h}_k (\mathbf{Y}_k^{\text{opt}} + \boldsymbol{\Psi}_k^{\text{opt}}) + \alpha_k^{\text{opt}} (\sigma_{\Delta}^2 \mathbf{h}_k \mathbf{I} + \mathbf{h}_k^* \mathbf{h}_k^T), \quad (50)$$

and $\boldsymbol{\Omega}_k^{\text{opt}} = \sum_{\ell \neq k} \boldsymbol{\Omega}_\ell^{\text{opt}}$. Note that in equation (49), all the constant terms have been omitted. In order for the problem in equation (49) to have a bounded value, it suffices to prove that matrix $\zeta^{\text{opt}} \mathbf{I} + \boldsymbol{\Omega}_k^{\text{opt}} - \frac{1}{\gamma_k} \boldsymbol{\Omega}_k^{\text{opt}}$ should be positive definite. Suppose that $\zeta^{\text{opt}} \mathbf{I} + \boldsymbol{\Omega}_k^{\text{opt}} - \frac{1}{\gamma_k} \boldsymbol{\Omega}_k^{\text{opt}}$ is not positive definite, then we can choose $\mathbf{W}_k = p \mathbf{w} \mathbf{w}^H$ where $p > 0$ and so the problem could be written as

$$\max_{\mathbf{W}_k \succeq \mathbf{0}} p \left(|\mathbf{a}^H(\theta_0) \mathbf{w}|^2 - \mathbf{w}^H \left(\zeta^{\text{opt}} \mathbf{I} + \boldsymbol{\Omega}_k^{\text{opt}} - \frac{1}{\gamma_k} \boldsymbol{\Omega}_k^{\text{opt}} \right) \mathbf{w} \right). \quad (51)$$

Now choose \mathbf{w} as a scaled multiple of one of the eigenvectors of $\zeta^{\text{opt}} \mathbf{I} + \boldsymbol{\Omega}_k^{\text{opt}} - \frac{1}{\gamma_k} \boldsymbol{\Omega}_k^{\text{opt}}$ associated with its negative eigenvalues. This means that, as per the definition of eigenvalues/eigenvectors, along with the negative definiteness assumption, we have that $\mathbf{w}^H \left(\zeta^{\text{opt}} \mathbf{I} + \boldsymbol{\Omega}_k^{\text{opt}} - \frac{1}{\gamma_k} \boldsymbol{\Omega}_k^{\text{opt}} \right) \mathbf{w} < 0$, this means that $|\mathbf{a}^H(\theta_0) \mathbf{w}|^2 - \mathbf{w}^H \left(\zeta^{\text{opt}} \mathbf{I} + \boldsymbol{\Omega}_k^{\text{opt}} - \frac{1}{\gamma_k} \boldsymbol{\Omega}_k^{\text{opt}} \right) \mathbf{w} > 0$ and so to maximize the entire cost appearing in equation (51), it suffices to take $p \rightarrow +\infty$, therefore the problem becomes unbounded above, which is a contradiction of the optimality of $\zeta^{\text{opt}}, \mathbf{a}^{\text{opt}}, \boldsymbol{\alpha}^{\text{opt}}, \boldsymbol{\Psi}^{\text{opt}}, \mathbf{Z}^{\text{opt}}$.

Now that we have positive definiteness of $\zeta^{\text{opt}} \mathbf{I} + \boldsymbol{\Omega}_k^{\text{opt}} - \frac{1}{\gamma_k} \boldsymbol{\Omega}_k^{\text{opt}}$, then there is a unique Hermitian positive definite matrix $\mathbf{R}_k^{\frac{1}{2}}$, such that $\zeta^{\text{opt}} \mathbf{I} + \boldsymbol{\Omega}_k^{\text{opt}} - \frac{1}{\gamma_k} \boldsymbol{\Omega}_k^{\text{opt}} = \mathbf{R}_k^{\frac{1}{2}} \mathbf{R}_k^{\frac{1}{2}}$ [31]. Using this square root matrix decomposition, we can express our cost in equation (49) as

$$\max_{\widetilde{\mathbf{W}}_k \succeq \mathbf{0}} \left(\mathbf{R}_k^{-\frac{1}{2}} \mathbf{a}(\theta_0) \right)^H \widetilde{\mathbf{W}}_k \left(\mathbf{R}_k^{-\frac{1}{2}} \mathbf{a}(\theta_0) \right) - \text{Tr} \left\{ \widetilde{\mathbf{W}}_k \right\}, \quad (52)$$

where $\widetilde{\mathbf{W}}_k = \mathbf{R}_k^{\frac{1}{2}} \mathbf{W}_k \mathbf{R}_k^{\frac{1}{2}}$. Now, suppose that the optimal solution, denoted hereby as $\widetilde{\mathbf{W}}_k^{\text{opt}}$, is not rank-one, i.e. $\text{rank } q > 1$. Then, employing the eigenvalue decomposition, we have that $\widetilde{\mathbf{W}}_k^{\text{opt}} = \sum_{n=1}^q \beta_n \widetilde{\mathbf{w}}_n \widetilde{\mathbf{w}}_n^H$ where $\beta_n \geq 0$ and $\|\widetilde{\mathbf{w}}_n\| = 1$, so the cost is upper bounded as follows

$$\begin{aligned} & \sum_{n=1}^q \beta_n \left| \left(\mathbf{R}_k^{-\frac{1}{2}} \mathbf{a}(\theta_0) \right)^H \widetilde{\mathbf{w}}_n \right|^2 - \sum_{n=1}^q \beta_n \\ & \leq \sum_{n=1}^q \beta_n \left| \left(\mathbf{R}_k^{-\frac{1}{2}} \mathbf{a}(\theta_0) \right)^H \widetilde{\mathbf{w}}_{\hat{n}} \right|^2 - \sum_{n=1}^q \beta_n, \end{aligned} \quad (53)$$

where we have upper bounded all terms by $\left| \left(\mathbf{R}_k^{-\frac{1}{2}} \mathbf{a}(\theta_0) \right)^H \widetilde{\mathbf{w}}_{\hat{n}} \right|^2$ where $\hat{n} = \arg \max_{n=1 \dots q} \left| \left(\mathbf{R}_k^{-\frac{1}{2}} \mathbf{a}(\theta_0) \right)^H \widetilde{\mathbf{w}}_n \right|^2$. But, this bound is achieved by the following rank-one contribution

$$\widetilde{\mathbf{W}}_k^{\text{rank-1}} = \left(\sum_{n=1}^q \beta_n \right) \widetilde{\mathbf{w}}_{\hat{n}} \widetilde{\mathbf{w}}_{\hat{n}}^H, \quad (54)$$

which is a contradiction of the assumption that $q > 1$. Therefore, $\widetilde{\mathbf{W}}_k^{\text{opt}}$ has to be rank-1 optimal. Now, since we have $\mathbf{W}_k^{\text{opt}} = \mathbf{R}_k^{-\frac{1}{2}} \widetilde{\mathbf{W}}_k^{\text{opt}} \mathbf{R}_k^{-\frac{1}{2}}$, we must also have that $\mathbf{W}_k^{\text{opt}}$ is rank-one optimal according to $\text{rank}(\mathbf{A}\mathbf{B}) \leq \min\{\text{rank}(\mathbf{A}), \text{rank}(\mathbf{B})\}$ and the proof is done.

APPENDIX B

SINGLE USER CLOSED-FORM SOLUTION

The following proof is trifold and goes as such:

A. Part 1: Optimal solution spans $\{\mathbf{a}^*(\theta_0), \mathbf{h}^*\}$

It is easy to see that when $\epsilon \rightarrow 0$, the problem in (31) converges to

$$(\mathcal{P}_6^{\text{SU}, \epsilon \rightarrow 0}) : \begin{cases} \max_{\mathbf{w}} & |\mathbf{a}^T(\theta_0) \mathbf{w}|^2 \\ \text{s.t.} & \gamma \sigma_c^2 - \sigma_{\Delta}^2 \|\mathbf{w}\|^2 \leq |\mathbf{h}^T \mathbf{w}|^2 \\ & \|\mathbf{w}\|^2 \leq 1 \end{cases} \quad (55)$$

First, we prove that the optimal solution of the above problem has to be a linear combination of $\mathbf{a}^*(\theta_0)$ and \mathbf{h}^* . In other words, $\mathbf{w}^{\text{opt}} \in \text{span}(\mathbf{a}^*(\theta_0), \mathbf{h}^*)$. To prove this, let us express any feasible \mathbf{w} as a decomposition of two vectors, namely

$$\mathbf{w} = \varphi \mathbf{w}_{\varphi} + \varrho \mathbf{w}_{\varrho}, \quad (56)$$

where $\|\mathbf{w}_{\varphi}\| = \|\mathbf{w}_{\varrho}\| = 1$, $\mathbf{w}_{\varphi} \perp \mathbf{w}_{\varrho}$ and $\mathbf{w}_{\varphi} \in \text{span}(\mathbf{a}^*(\theta_0), \mathbf{h}^*)$, i.e. \mathbf{w}_{ϱ} lies in the null space of $\text{span}(\mathbf{a}^*(\theta_0), \mathbf{h}^*)$. Note that ϱ does not contribute to an increase in the cost because $\mathbf{a}^T(\theta_0) \mathbf{w}_{\varrho} = 0$. Therefore, cost maximization is attained by increasing φ , only. Next, a feasible solution in terms of ϱ, φ should satisfy

$$\gamma \sigma_c^2 - \sigma_{\Delta}^2 (\varphi^2 + \varrho^2) \leq \varphi^2 |\mathbf{h}^T \mathbf{w}_{\varphi}|^2, \quad (57)$$

and

$$\varphi^2 + \varrho^2 \leq 1, \quad (58)$$

where the upper bound in (57) appears due to $\mathbf{h}^T \mathbf{w}_{\varrho} = 0$. For a given set of parameters, $(\gamma, \sigma_c^2, \sigma_{\Delta}^2)$, it can be easily seen that an increase in φ would only increase the gap between the two bounds in the constraint appearing in equation (57). Therefore, to sum things up, an increase of φ only would increase the cost, while preserving feasibility of the solution. Therefore, to achieve the most out of the problem, one could choose $\varphi = 1$ and $\varrho = 0$, which means that \mathbf{w} lives in the subspace spanned by $\mathbf{a}^*(\theta_0)$ and \mathbf{h}^* .

B. Part 2: Optimal solution expressed in $\{\mathbf{a}_{\parallel}, \mathbf{a}_{\perp}\}$

Now that we proved that the optimal solution is within $\text{span}(\mathbf{a}^*(\theta_0), \mathbf{h}^*)$, then let's consider an orthonormal representation of that subspace, which could be done via the Gram-Schmidt process, i.e. let's pick the axis of reference first to be $\mathbf{a}^*(\theta_0)$, i.e.

$$\mathbf{a}_{\parallel} = \frac{\mathbf{a}^*(\theta_0)}{\|\mathbf{a}(\theta_0)\|} \quad (59)$$

$$\mathbf{a}_{\perp} = \frac{\mathbf{h}^* - \mathbf{a}_{\parallel}^H \mathbf{h}^* \mathbf{a}_{\parallel}}{\|\mathbf{h}^* - \mathbf{a}_{\parallel}^H \mathbf{h}^* \mathbf{a}_{\parallel}\|}. \quad (60)$$

Let the optimal solution in this case be written as

$$\mathbf{w}^{\text{opt}} = \alpha_{\parallel} \mathbf{a}_{\parallel} + \alpha_{\perp} \mathbf{a}_{\perp}. \quad (61)$$

Replacing this representation in the optimization problem of equation (55), we get

$$(\mathcal{P}_6^{\text{SU}, \epsilon \rightarrow 0}) : \begin{cases} \max_{\alpha_{\parallel}, \alpha_{\perp}} & |\alpha_{\parallel}|^2 \overbrace{|\mathbf{a}^T(\theta_0) \mathbf{a}_{\parallel}|^2}^N \\ \text{s.t.} & \gamma \sigma_c^2 - \sigma_{\Delta}^2 (|\alpha_{\parallel}|^2 + |\alpha_{\perp}|^2) \leq |\mathbf{h}^T \mathbf{w}^{\text{opt}}|^2 \\ & |\alpha_{\parallel}|^2 + |\alpha_{\perp}|^2 \leq 1 \end{cases} \quad (62)$$

It is clear that from the above, the cost function increases as a function of $|\alpha_{\parallel}|^2$, with no contribution from α_{\perp} . To satisfy the unit circle constraint, take $|\alpha_{\parallel}|^2 = 1$ and $|\alpha_{\perp}|^2 = 0$. Now, so that this solution, namely $\mathbf{w}^{\text{opt}} = \mathbf{a}_{\parallel}$ is optimal, the first constraint in problem (62) needs to be feasible, that is

$$\gamma \sigma_c^2 - \sigma_{\Delta}^2 \leq |\mathbf{h}^T \mathbf{a}_{\parallel}|^2. \quad (63)$$

Using the representation of \mathbf{a}_{\parallel} in equation (59), the condition in equation (63) becomes

$$N(\gamma \sigma_c^2 - \sigma_{\Delta}^2) \leq |\mathbf{h}^T \mathbf{a}^*(\theta_0)|^2. \quad (64)$$

Also note that by Cauchy-Schwarz, we have that $N(\gamma\sigma_c^2 - \sigma_\Delta^2) \leq \|\mathbf{h}\|^2 N$, hence the factor $\frac{\gamma\sigma_c^2 - \sigma_\Delta^2}{\|\mathbf{h}\|^2} \leq 1$, which gives us a bound on the choice of parameters $(\gamma, \sigma_\Delta, \sigma_c^2)$ as $\gamma \leq \frac{\|\mathbf{h}\|^2 + \sigma_\Delta^2}{\sigma_c^2}$, which also happens to be the upper bound on single user average-SINR, under a unit power budget constraint on \mathbf{w} . Indeed

$$\begin{aligned} \max_{\|\mathbf{w}\|=1} \mathbb{E}\{\text{SINR}\} &= \max_{\|\mathbf{w}\|=1} \frac{\mathbf{w}^H \mathbb{E}\{\tilde{\mathbf{h}} \tilde{\mathbf{h}}^T\} \mathbf{w}}{\sigma_c^2} \\ &= \max_{\|\mathbf{w}\|=1} \frac{\mathbf{w}^H (\mathbf{h}^* \mathbf{h}^T + \sigma_\Delta^2 \mathbf{I}) \mathbf{w}}{\sigma_c^2} \quad (65) \\ &= \frac{\|\mathbf{h}\|^2 + \sigma_\Delta^2}{\sigma_c^2}, \end{aligned}$$

where the last step is by choosing \mathbf{w} to be the eigenvector corresponding to the maximum eigenvalue of $\mathbf{h}^* \mathbf{h}^T + \sigma_\Delta^2 \mathbf{I}$.

C. Part 3: Optimal solution expressed in $\{\mathbf{h}_\parallel, \mathbf{h}_\perp\}$

Using the same approach as in Appendix B-B, we consider an orthonormal representation of the subspace $\text{span}(\mathbf{a}^*(\theta_0), \mathbf{h}^*)$, but instead we now pick the reference to be \mathbf{h}^* , viz.

$$\mathbf{h}_\parallel = \frac{\mathbf{h}^*}{\|\mathbf{h}\|} \quad (66)$$

$$\mathbf{h}_\perp = \frac{\mathbf{a}^*(\theta_0) - \mathbf{h}_\parallel^H \mathbf{a}^*(\theta_0) \mathbf{h}_\parallel}{\|\mathbf{a}^*(\theta_0) - \mathbf{h}_\parallel^H \mathbf{a}^*(\theta_0) \mathbf{h}_\parallel\|}, \quad (67)$$

and so the solution takes the form

$$\mathbf{w}^{\text{opt}} = \alpha_1 \mathbf{h}_\parallel + \alpha_2 \mathbf{h}_\perp. \quad (68)$$

Replacing this representation in the optimization problem of equation (69), we get

$$(\mathcal{P}_6^{\text{SU}, \epsilon \rightarrow 0}) : \begin{cases} \max_{\alpha_1, \alpha_2} & |\alpha_1 \mathbf{a}^T(\theta_0) \mathbf{h}_\parallel + \alpha_2 \mathbf{a}^T(\theta_0) \mathbf{h}_\perp|^2 \\ \text{s.t.} & \gamma\sigma_c^2 - \sigma_\Delta^2 (|\alpha_1|^2 + |\alpha_2|^2) \leq |\alpha_1|^2 \|\mathbf{h}\|^2 \\ & |\alpha_1|^2 + |\alpha_2|^2 \leq 1. \end{cases} \quad (69)$$

It is clear that the cost is maximized upon adjusting the phases of α_1, α_2 as follows

$$\exp(j\angle\alpha_1) = \exp\{-j\angle(\mathbf{a}^T(\theta_0) \mathbf{h}_\parallel)\} = \frac{\mathbf{h}_\parallel^H \mathbf{a}^*(\theta_0)}{\|\mathbf{h}_\parallel^H \mathbf{a}^*(\theta_0)\|} \quad (70)$$

$$\exp(j\angle\alpha_2) = \exp\{-j\angle(\mathbf{a}^T(\theta_0) \mathbf{h}_\perp)\} = \frac{\mathbf{h}_\perp^H \mathbf{a}^*(\theta_0)}{\|\mathbf{h}_\perp^H \mathbf{a}^*(\theta_0)\|}. \quad (71)$$

In that case, both complex numbers $\alpha_1 \mathbf{a}^T(\theta_0) \mathbf{h}_\parallel$ and $\alpha_2 \mathbf{a}^T(\theta_0) \mathbf{h}_\perp$ add up constructively. Then, it is clear that the gains $|\alpha_1|$ and $|\alpha_2|$ should be jointly maximized, therefore, the last constraint should be attained with equality, i.e. $|\alpha_1|^2 + |\alpha_2|^2 = 1$. In that case, the first constraint translates to $1 \geq |\alpha_1|^2 \geq \rho$ and $|\alpha_2|^2 \leq 1 - \rho \leq 1$, where

$$0 \leq \rho \triangleq \frac{\gamma\sigma_c^2 - \sigma_\Delta^2}{\|\mathbf{h}\|^2} \leq 1, \quad (72)$$

which is satisfied upon $\gamma \leq \frac{\|\mathbf{h}\|^2 + \sigma_\Delta^2}{\sigma_c^2}$. Once $|\alpha_1|$ and $|\alpha_2|$ are set, then we have an optimal solution. Working in the compliment region of that defined in equation (64), i.e.

$$N(\gamma\sigma_c^2 - \sigma_\Delta^2) > |\mathbf{h}^T \mathbf{a}^*(\theta_0)|^2, \quad (73)$$

or equivalently $|\mathbf{a}^T(\theta_0) \mathbf{h}_\parallel|^2 \leq N\rho$. Also since $\mathbf{h}_\parallel, \mathbf{h}_\perp$ form an orthonormal basis in $\text{span}(\mathbf{a}^*(\theta_0), \mathbf{h}^*)$, which means $|\mathbf{a}^T(\theta_0) \mathbf{h}_\parallel|^2 + |\mathbf{a}^T(\theta_0) \mathbf{h}_\perp|^2 = \|\mathbf{a}^T(\theta_0)\|^2 = N$. Based on this argument, one also has $|\mathbf{a}^T(\theta_0) \mathbf{h}_\perp|^2 \geq N(1 - \rho)$. It could be shown that by the choice

of $|\alpha_1|^2 = \rho$ and so $|\alpha_2|^2 = 1 - \rho$ maximizes the cost. Finally, the optimal solution is

$$\mathbf{w}^{\text{opt}} = \underbrace{\sqrt{\rho} \frac{\mathbf{h}_\parallel^H \mathbf{a}^*(\theta_0)}{\|\mathbf{h}_\parallel^H \mathbf{a}^*(\theta_0)\|}}_{\alpha_1} \mathbf{h}_\parallel + \underbrace{\sqrt{1 - \rho} \frac{\mathbf{h}_\perp^H \mathbf{a}^*(\theta_0)}{\|\mathbf{h}_\perp^H \mathbf{a}^*(\theta_0)\|}}_{\alpha_2} \mathbf{h}_\perp. \quad (74)$$

ACKNOWLEDGMENT

The authors would like to thank Dr. Lasha Ephremidze and Prof. Ilya Spitkovsky of the NYU Abu Dhabi Mathematics department for help with the proofs of the theorems appearing in this manuscript, regarding rank — one optimality and closed-form solutions for the SU case. Also, simulations were conducted on NYU Abu Dhabi's HPC Jubail Cluster.

REFERENCES

- [1] T. Hewa, G. Gür, A. Kalla, M. Ylianttila, A. Bracken and M. Liyanage, "The Role of Blockchain in 6G: Challenges, Opportunities and Research Directions," *2020 2nd 6G Wireless Summit (6G SUMMIT)*, 2020, pp. 1-5, doi: 10.1109/6GSUMMIT49458.2020.9083784.
- [2] W. Saad, M. Bennis, and M. Chen, "A vision of 6G wireless systems: Applications, trends, technologies, and open research problems," *IEEE Network*, vol. 34, no. 3, pp. 134–142, May/June 2020.
- [3] W. Tong and P. Zhu, *6G: The Next Horizon: From Connected People and Things to Connected Intelligence*. Cambridge, U.K.: Cambridge Univ. Press, 2021.
- [4] D. Ma, N. Shlezinger, T. Huang, Y. Liu and Y. C. Eldar, "Joint Radar-Communication Strategies for Autonomous Vehicles: Combining Two Key Automotive Technologies," in *IEEE Signal Processing Magazine*, vol. 37, no. 4, pp. 85-97, July 2020, doi: 10.1109/MSP.2020.2983832.
- [5] A. R. Chiriyath, B. Paul and D. W. Bliss, "Radar-Communications Convergence: Coexistence, Cooperation, and Co-Design," in *IEEE Transactions on Cognitive Communications and Networking*, vol. 3, no. 1, pp. 1-12, March 2017, doi: 10.1109/TCCN.2017.2666266.
- [6] B. Paul, A. R. Chiriyath and D. W. Bliss, "Survey of RF Communications and Sensing Convergence Research," in *IEEE Access*, vol. 5, pp. 252-270, 2017, doi: 10.1109/ACCESS.2016.2639038.
- [7] L. Zheng, M. Lops, Y. C. Eldar, and X. Wang, "Radar and Communication Coexistence: An Overview: A Review of Recent Methods," *IEEE Signal Processing Magazine*, vol. 36, no. 5, pp. 85-99, September 2019.
- [8] C. B. Barneto et al., "Full Duplex Radio/Radar Technology: The Enabler for Advanced Joint Communication and Sensing," in *IEEE Wireless Communications*, vol. 28, no. 1, pp. 82-88, February 2021, doi: 10.1109/MWC.001.2000220.
- [9] H. Griffiths et al., "Radar Spectrum Engineering and Management: Technical and Regulatory Issues," in *Proceedings of the IEEE*, vol. 103, no. 1, pp. 85-102, Jan. 2015, doi: 10.1109/JPROC.2014.2365517.
- [10] B. Li, A. P. Petropulu and W. Trappe, "Optimum Co-Design for Spectrum Sharing between Matrix Completion Based MIMO Radars and a MIMO Communication System," in *IEEE Transactions on Signal Processing*, vol. 64, no. 17, pp. 4562-4575, 1 Sept.1, 2016, doi: 10.1109/TSP.2016.2569479.
- [11] M. Kobayashi, G. Caire and G. Kramer, "Joint State Sensing and Communication: Optimal Tradeoff for a Memoryless Case," 2018 *IEEE International Symposium on Information Theory (ISIT)*, 2018, pp. 111-115, doi: 10.1109/ISIT.2018.8437621.
- [12] A. R. Chiriyath, B. Paul, G. M. Jacyna and D. W. Bliss, "Inner Bounds on Performance of Radar and Communications Co-Existence," in *IEEE Trans. Signal Process.*, vol. 64, no. 2, pp. 464-474, Jan.15, 2016, doi: 10.1109/TSP.2015.2483485.
- [13] M. Gastpar, M. Vetterli and P. L. Dragotti, "Sensing reality and communicating bits: a dangerous liaison," in *IEEE Signal Processing Magazine*, vol. 23, no. 4, pp. 70-83, July 2006, doi: 10.1109/MSP.2006.1657818.
- [14] C. Sturm and W. Wiesbeck, "Waveform Design and Signal Processing Aspects for Fusion of Wireless Communications and Radar Sensing," in *Proceedings of the IEEE*, vol. 99, no. 7, pp. 1236-1259, July 2011, doi: 10.1109/JPROC.2011.2131110.
- [15] K. V. Mishra, M. R. Bhavani Shankar, V. Koivunen, B. Ottersten and S. A. Vorobyov, "Toward Millimeter-Wave Joint Radar Communications: A Signal Processing Perspective," in *IEEE Signal Processing Magazine*, vol. 36, no. 5, pp. 100-114, Sept. 2019, doi: 10.1109/MSP.2019.2913173.

- [16] N. Su, F. Liu, and C. Masouros, "Secure radar-communication systems with malicious targets: Integrating radar, communications and jamming functionalities," *IEEE Trans. Wireless Commun.*, vol. 20, no. 1, pp. 83–95, Jan. 2021.
- [17] F. Liu, C. Masouros, A. Li, and T. Ratnarajah, "Robust MIMO beamforming for cellular and radar coexistence," *IEEE Wireless Commun. Lett.*, vol. 6, no. 3, pp. 374–377, Jun. 2017.
- [18] M. F. Keskin, V. Koivunen, and H. Wymeersch, "Limited feedforward waveform design for OFDM dual-functional radar-communications," *IEEE Transactions on Signal Processing*, vol. 69, pp. 2955–2970, 2021.
- [19] Y. Chen, M. Wen, L. Wang, W. Liu, and L. Hanzo, "SINR-outage minimization of robust beamforming for the non-orthogonal wireless downlink," *IEEE Transactions on Communications*, vol. 68, no. 11, pp. 7247–7257, Nov. 2020.
- [20] N. Vucic and H. Boche, "Robust QoS-constrained optimization of downlink multiuser MISO systems," *IEEE Transactions on Signal Processing*, vol. 57, no. 2, pp. 714–725, Feb. 2009.
- [21] H. Chen, H. Saeeddein, T. Ballal, H. Wymeersch, M. -S. Alouini and T. Y. Al-Naffouri, "A Tutorial on Terahertz-Band Localization for 6G Communication Systems," in *IEEE Communications Surveys & Tutorials*, doi: 10.1109/COMST.2022.3178209.
- [22] I. Bechar, "A Bernstein-type inequality for stochastic processes of quadratic forms of Gaussian variables." Available: <http://arxiv.org/abs/0909.3595>
- [23] Zou, Y., Long, Y., Gong, S., Hoang, D.T., Liu, W., Cheng, W. and Niyato, D., "Robust Beamforming Optimization for Self-Sustainable Intelligent Reflecting Surface Assisted Wireless Networks," *IEEE Transactions on Cognitive Communications and Networking*, vol. 8, no. 2, pp. 856–870, Aug. 2022.
- [24] F. Liu, L. Zhou, C. Masouros, A. Li, W. Luo, and A. Petropulu, "Toward dual-functional radar-communication systems: Optimal waveform design," *IEEE Trans. Signal Process.*, vol. 66, no. 16, pp. 4264–4279, Aug. 2018.
- [25] J. A. Zhang, F. Liu, C. Masouros, R. W. Heath, Z. Feng, L. Zheng, and A. Petropulu, "An overview of signal processing techniques for joint communication and radar sensing," *IEEE Journal of Selected Topics in Signal Process.*, pp. 1–1, 2021.
- [26] K.-Y. Wang, *et al.*, "Outage constrained robust transmit optimization for multiuser MISO downlinks: Tractable approximations by conic optimization," *IEEE Transactions on Signal Processing*, vol. 62, no. 21, pp. 5690–5705, Nov. 2014.
- [27] S. Ma and D. Sun, "Chance constrained robust beamforming in cognitive radio networks," *IEEE Commun. Lett.*, vol. 17, no. 1, pp. 67–70, Jan. 2013.
- [28] G. Zheng, K. Wong, A. Paulraj, and B. Ottersten, "Robust collaborative relay beamforming," *IEEE Transactions on Signal Processing*, vol. 57, no. 8, Aug. 2009.
- [29] X. Hu, C. Masouros, F. Liu, and R. Nessel. "MIMO-OFDM Dual-Functional Radar-Communication Systems: Low-PAPR Waveform Design." *arXiv preprint arXiv:2109.13148* (2021).
- [30] H. Xu, R. Blum, J. Wang, and J. Yuan, "Collocated MIMO radar waveform design for transmit beam pattern formation," *IEEE Trans. Aerosp. Electron. Syst.*, vol. 51, no. 2, pp. 1558–1568, Apr. 2015.
- [31] R. A. Horn and C. R. Johnson, *Matrix Analysis*. Cambridge, U.K.: Cambridge Univ. Press, 1987.
- [32] M. Grant, S. Boyd, and Y. Ye. (2008). *CVX: MATLAB Software for Disciplined Convex Programming*. [Online]. Available: <http://cvxr.com/cvx/>
- [33] A. Khawar, A. Abdelhadi, and C. Clancy, "Target detection performance of spectrum sharing MIMO radars," *IEEE Sensors J.*, vol. 15, no. 9, pp. 4928–4940, Sep. 2015.
- [34] Z. Cheng, C. Han, L. Bin, Z. He, and J. Li, "Communication-aware waveform design for MIMO radar with good transmit beam pattern," *IEEE Trans. Signal Process.*, vol. 66, no. 21, pp. 5549–5562, Nov. 2018.